UNIVERSITA' DEGLI STUDI DI PADOVA

Dipartimento di Scienze Chirurgiche, Oncologiche e Gastroenterologiche

SCUOLA DI DOTTORATO DI RICERCA IN

ONCOLOGIA E ONCOLOGIA CHIRURGICA

XXV CICLO

SELECTIVE TARGETING OF NOTCH-1 FOR THERAPEUTIC PURPOSES IN XENOGRAFT MODELS OF T-ACUTE LYMPHOBLASTIC LEUKEMIA

Direttore della Scuola : Ch.ma Prof.ssa Paola Zanovello

Supervisore : Dr. Stefano Indraccolo

Dottoranda: Dott.ssa Valentina Agnusdei

INDEX

RIASSUNTO

La leucemia linfoblastica acuta a cellule T (T-ALL) è una malattia eterogenea caratterizzata da diverse alterazioni genetiche e caratteristiche cliniche, sia in età pediatrica che adulta. Un ruolo importante in questo tipo di neoplasia è ricoperto dal pathway di Notch, meccanismo evolutivamente conservato coinvolto in numerosi processi biologici tra cui il differenziamento dei linfociti T; difatti in circa il 50-55% dei pazienti affetti da T-ALL si riscontra una mutazione attivante nel gene *NOTCH1* o a carico di *FBW7*. Dal momento che solo il 70-80% dei bambini e il 40% degli adulti affetti da questo tipo di leucemia riesce a raggiungere la remissione a lungo termine, e' necessario sviluppare ed adottare nuove strategie terapeutiche per poter curare anche i pazienti refrattari alle terapie convenzionali. A questo scopo abbiamo analizzato gli effetti biologici e terapeutici di un anticorpo neutralizzante specifico per il recettore Notch1 umano, avvalendoci di un modello di xenotrapianto di T-ALL. Tale modello è stato generato nel nostro laboratorio utilizzando campioni ottenuti da pazienti pediatrici con caratteristiche cliniche differenti e presentanti diverso stato mutazionale di *NOTCH1/FBW7*. Il trattamento con anti-Notch1 si è rivelato efficace nel contrastare la crescita della leucemia dei campioni con mutazione di *NOTCH1/FBW7*, compresi campioni derivati da pazienti in ricaduta o poco responsivi alle terapie convenzionali. In seguito alla somministrazione di anti-Notch1, in questi xenotrapianti abbiamo osservato un aumento dei livelli di apoptosi, una riduzione della proliferazione, un effetto inibitorio molto marcato sui profili trascrizionali dei geni target di Notch e inoltre una modulazione del metabolismo cellulare delle cellule leucemiche. Gli esperimenti di inoculo seriale indicano che la terapia con anti-Notch1 può compromettere la capacità di dare origine a leucemia delle cellule di T-ALL residue dopo il trattamento. Inoltre un esperimento preliminare ha rivelato che la somministrazione continua dell'anticorpo anti-Notch1 può causare l'insorgenza di fenomeni di resistenza alla terapia. Infine abbiamo dimostrato che la combinazione di anti-Notch1 e

desametasone, un farmaco comunemente utilizzato nel trattamento delle T-ALL, può ulteriormente migliorare l'efficacia terapeutica.

Nel complesso, i nostri risultati indicano che la presenza di mutazioni in *NOTCH1/FBW7* identifica dei candidati che potrebbero beneficiare di una terapia mirata contro Notch1 e sottolinea la potenzialità del valutare l'espressione dei geni target di Notch e del CD7 come marcatori predittivi della risposta terapeutica all'anti-Notch1.

ABSTRACT

T-cell acute lymphoblastic leukemia (T-ALL) is an heterogeneous disease, characterized by several genetic alterations and polymorphic clinical features both in children and adults. The Notch pathway, an evolutionary conserved pathway involved in many biological processes including T cell differentiation, has been implicated in the pathogenesis of this disease. Notably, about 50-55% of T-ALL samples show increased Notch1 activity, due to mutations in *NOTCH1* or *FBW7* genes. Among T-ALL patients, only 70-80% of children and 40% of adults reach long-term remission, therefore new therapeutic approaches are required. Here, we investigated the biologic and therapeutic effects of a human Notch1-specific neutralizing antibody in xenograft models of pediatric T-ALL, obtained from patients with different clinical features and *NOTCH1/FBW7* mutational status. We demonstrated that anti-Notch1 treatment greatly delayed engraftment of T-ALL cells bearing *NOTCH1/FBW7* mutations, including samples derived from relapsed and clinically difficult-to-treat patients. In these xenografts we observed increased levels of apoptosis, decreased proliferation of leukemic cells and a marked inhibitory effects on Notch transcriptional profile. Moreover, modulation of T-ALL cells metabolism was detected following anti-Notch1 therapy. Serial transplantation experiments suggested that anti-Notch1 therapy could compromise leukemia initiating cell functions and a preliminary experiment showed that resistance may arise in a regimen of continuous administration of anti-Notch1 mAb. Finally, we demonstrated that combination of anti-Notch1 and dexamethasone – a leading drug in T-ALL treatment - could further improve therapeutic effect.

Altogether these results indicate that *NOTCH1/FBW7* mutations identify suitable candidates for Notch targeted therapy and highlight the potential of Notch target genes and CD7 expression as candidate predictive markers of response to anti-Notch1 therapy.

1. INTRODUCTION

1.1 T-CELL ACUTE LYMPHOBLASTIC LEUKEMIA

1.1.1 Molecular pathogenesis of T-ALL

T-cell acute lymphoblastic leukemia (T-ALL) is an hematologic disease induced by the transformation of T-cell progenitors. T-ALL are approximately 15% and 25% of the newly diagnosed cases of ALL in children and in adults, respectively. Compared to the more common B-cell-lineage ALL, T-ALL is associated with more unfavorable clinical features, such as a high white-blood-cell count, bulky adenopathy, involvement of the central nervous system and is linked with a poor prognosis. The onset of T-ALL is due to transformation events that arise in crucial steps of intrathymic T-cell differentiation and expression of certain oncogenes has been closely linked to developmental arrest at particular stages of normal thymocytes development (Aifantis et al., 2008). Each stage of maturation is accompanied by a distinct pattern of intracellular and cell surface markers so the immunophenotype analysis provides the basis for the commonly used EGIL (European Group for the Immunological Characterization of Leukemias) classification system. Also T-cell receptor based classification system reflect stages of physiological development but it is less widely used in the clinical practice (Fielding et al., 2012).

Current knowledge of T-ALL biology entails five key issues:

- Chromosomal aberrations: approximately 50% of T-ALL cases have chromosome aberrations but T-ALL cytogenetics is not well understood as occurs in B-ALL, where cytogenetic analysis is used to draw therapeutic decisions. Chromosomal aberrations in T-ALL can be divided into three categories. The first includes rearrangements of proto-oncogenes to *TCR* gene locus, leading to overexpression of rearranged proto-oncogenes (such

as *LMO1, LMO2, TAL1*). The second includes rearrangements of transcription factors-coding genes, resulting in the production of aberrant fusion transcription factors (for example *STIL-TAL1*, *TLX3-BCL11B*). The third concerns rearrangements of the *MLL* gene to different translocation partner genes. Some of the transcription factors involved in rearrangements are normally expressed in non-malignant thymocytes and are essential regulators of T-cell development, whereas others are ectopically expressed by transformed cells in T-ALL and not expressed in normal thymus. These chromosomal translocations cause aberrant patterns of gene expression in T-cells and lead to abnormal cell-cycle control, proliferation and differentiation (Aifantis et al., 2008; Kraszewska et al., 2012b).

- Gene expression profiles: most T-ALL patients show pathological gene expression even in the absence of chromosome aberrations. It was demonstrated that T-ALL patients cluster into several groups characterized by differential gene expression patterns (Ferrando et al., 2002). Patients could be divided into four groups based on the aberrant, subtype-specific, expression of *TLX1*, *LYL1*, *TAL1/LMO2* and *TLX3* oncogenes. *TLX1* encodes a transcription factor belonging to the homeobox family with a role in T-ALL pathogenesis highlighted by different studies. *LYL1* and *TAL1* are two related basic helix-loop-helix genes expressed in hematopoietic and endothelial lineages. *TAL1* is essential for hematopoietic and vascular development whereas *LYL1* seems to act mainly in adult neovasculatization (Pirot et al., 2010). *LMO2* codes for a transactivating protein that has activity in erythropoiesis and leukemogenesis. *TAL1* and *LMO2* are found simultaneously overexpressed in the same samples so these two genes characterize one T-ALL subtype. Finally, *TLX3* encodes a homeobox transcription factor found to be involved in T-ALL pathogenesis, whether or not a chromosome translocation was detected (Kraszewska et al., 2012b). Overexpression of *HOXA* genes was further proposed as a factor defining a separate T-ALL

subtype (Dik et al., 2005). The number of T-ALL subtypes defined by gene expression profiling data is quite limited, considering that 50% of T-ALL patients carry chromosomal aberrations. A possible explanation is that various molecular aberrations can lead to overexpression of the same oncogenes. Recently a novel T-ALL subtype, characterized by a distinct gene expression profile, expression of specific cell surface antigens and increased number of genetic alterations, has been identified. This subtype is named early T-cell precursor leukemia (ETP-ALL), arises from stem cell-like precursors of thymocytes and is associated with a very poor prognosis (Coustan-Smith et al., 2009). In addition to genome wide gene expression analysis, recent studies have described T-ALL-specific miRNA expression profiles (Mavrakis et al., 2011).

- Gene mutations: additional genetic abnormalities observed in T-ALL include mutations in *NOTCH1* and *FBW7* genes - which will be described later – and the new candidate genes involved in T-ALL pathogenesis *FLT3*, *BCL11B*, *PTPN2*, *PHF6*, *NRAS*, *WT1*, *CDKN2A* and *IL7R*. The discovery of these genes has contributed to the knowledge about T-ALL biology but none of them have proved so far to have prognostic value.

- Immunoglobulin and T-cell receptor (*Ig/TCR*) gene rearrangements, including Ig/TCR- based monitoring of minimal residual disease (MRD): during lymphocyte maturation, rearrangement of the TCR loci occurs, in order to generate the T cell diversity required for an appropriate immune response. This process is mediated by a recombinase enzyme complex which randomly joins unique V, D, J gene segments together to form various combinations. Rearrangement diversity is further increased by small deletions and insertions of nucleotide mediated by terminal deoxynucleotidyl transferase (TDT). Every lymphocyte clone, including leukemic clones, carry unique *Ig/TCR* gene rearrangements so the study of rearrangement pattern might be used for immunogenetic characteristics of T-ALL, as indicators of clonality in diagnosis of lymphoproliferative disorders and for monitoring the MRD. The recombination events that

occur during T cell development require that the thymocyte DNA be inclined to breakage and rejoining, causing lymphocyte-specific genetic instability and so supporting the process of malignant transformation. In normal T cells only *TCR* rearrangements occur, however in 20% of T-ALL cases there is also an incomplete immunoglobulin heavy chain rearrangement, caused by a high activity of recombinase in leukemic cells and abnormal *Ig/TCR* locus accessibility due to uncontrolled cell proliferation. *Ig/TCR* gene rearrangements reflect the stage of T-cell precursor that undergoes leukemic transformation. *Ig/TCR* gene rearrangements are investigated for clinical reasons but they are not related to the oncogenic process. The level of MRD has revealed to be the most reliable prognostic marker in T-ALL, as explained it the last section.

- DNA methylation: the few studies existing so far on methylation status in T-ALL demonstrate that DNA methylation of particular genes, such as *PTEN*, is different between T-ALL patients, healthy children and normal thymic cell populations. However, these results need to be confirmed in large prospective studies (Roman-Gomez et al., 2005) (Kraszewska et al., 2012a).

Gene mutations, chromosome rearrangements and oncogene overexpression can be linked as mechanisms leading to a disruption of cellular pathways controlling lymphocyte differentiation and proliferation (Kraszewska et al., 2012b).

1.1.2 Overview of T-cell development

Initiation of lymphoid commitment is not fully understood, with several haematopoietic-cell populations being proposed as lymphocytes progenitors. Nevertheless, the cells that are committed to become T-cells exit the bone marrow and migrate through the blood to the thymus in a chemotactic process that is controlled by adhesion molecules. The microenvironment in the thymus allows development of multi-potential progenitors and correct maturation of T-cells. The first precursors that migrate to the thymus are early T-cell-lineage progenitors

(ETPs) or double negative 1 (DN1) cells, phenotypically belonging to a $CD3^-$ $CD4^{-/low}$ $CD8^-CD25^-CD44^{hi}KIT^+$ fraction. In the T lineage commitment, they first down-regulate KIT expression, thus becoming $CD4^-CD8^-CD25^+CD44^+$ DN2 cells, then CD44, becoming DN3 cells $CD4^-CD8^-CD25^+CD44^-$, and finally CD25, becoming DN4 cells $CD4^-CD8^-CD25^-CD44^-$. During these events, T-cells progenitors remain in intimate contact with thymic epithelial stromal cells. This contact is essential because stromal cells express Notch ligands and produce growth factors and morphogenes that control T-progenitors development. Upon pre-T-cell receptor (pre-TCR) engagement, thymocytes differentiate into double positive (DP, $CD4^+CD8^+$) cells, that enter the processes of positive and negative selection. Selected T-cells exit the thymus as mature single positive (SP) $CD4^+$ or $CD8^+$ cells (Aifantis et al., 2008) (Fig. 1). Different pathways contribute to drive T cell development, in particular Notch signaling has a critical role as explained in the next section.

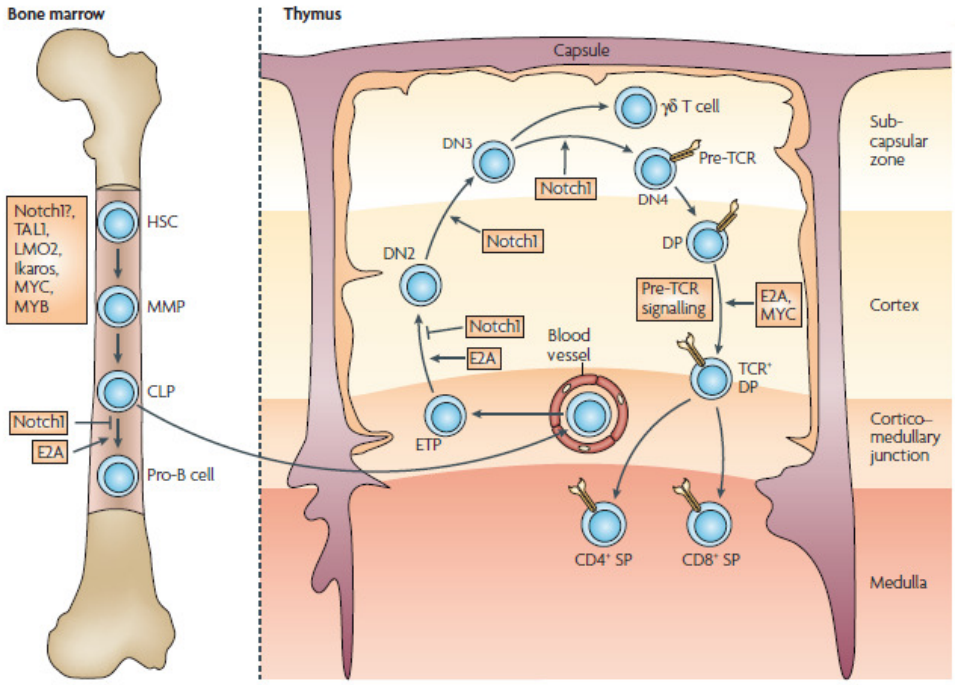

Figure 1: Stages of haematopoiesis and T-cell development: Outline of the T-cell development, from haematopoietic stem cells (HSCs) to multipotent progenitors (MPPs) and to common lymphoid progenitors (CLPs). These subsets migrate from the bone marrow to the thymus as early T-cell-lineage progenitors (ETPs) and commit to the T-cell lineage, progressing through the double negative stages DN2, DN3, DN4. When pre-TCR-selected cells reach the double positive (DP) stage, they are subjected to the positive and negative selection. Selected cells exit the thymus as single positive (SP) $CD4^+$ or $CD8^+$ T-cells. Oncogenes, including Notch1, that are known to be associated with T-ALL are reported (Aifantis et al., 2008).

1.2 NOTCH

1.2.1 Notch signaling

Notch is a key regulator of different cellular processes, such as differentiation, proliferation, apoptosis, adhesion and spatial development. Mammals have four Notch receptors (Notch1-Notch4) and five Notch ligands (JAG1, JAG2, DLL1, DLL3, DLL4), all of which are single-pass transmembrane proteins so Notch pathway functions as a mediator of short-range cell-cell communication. Notch proteins are first synthesized as single-pass transmembrane glycoproteins of 300-350 kDa, which are later proteolytically processed in the Golgi by a furin-like convertase at a site called S1. This processing generates two noncovalently associated subunits, the extracellular Notch (N_{EC}) and the transmembrane Notch (N_{TM}), which constitute the mature heterodimeric form of the receptor present at the cell surface. The extracellular domain contains a variable number (29-36) of N-terminal epidermal growth factor (EGF)-like repeats that include the ligands-binding region. Beyond the EGF-like repeats there is a negative regulatory region (NRR) containing three LNR modules (LIN12/Notch repeats), which contribute to avoid premature activation of Notch receptors. The transmembrane subunit contains a short extracellular region, a transmembrane segment and an intracellular region (ICN), which is further divided in a RAM (RBPJ-associated module) domain, six/seven ankyrin (ANK) repeats flanked by two nuclear localization signals (NLSs), a transactivation domain (TAD) and a PEST region. The ANK and RAM domains participate to the binding of the transcription factor RBPJ or CSL while the ANK domain is essential for recruitment of co-activators and transactivation. The NLSs sequences allow the nuclear localization of the intracellular region, TAD is the transactivation domain and the PEST sequence (proline-glutamic acid-serine-threonine-rich domain) is essential for protein stability and for its proteasome-mediated degradation. Ligands are members of the DSL (Delta, Serrate and LAG2) family, they are transmembrane proteins containing a transmembrane domain, a small cytoplasmic tail, variable numbers of

EGF-like repeats and a DSL domain essential for binding to the EGF-like domain in the Notch extracellular subunit (fig. 2) (Kopan and Ilagan, 2009; Sanchez-Irizarry et al., 2004).

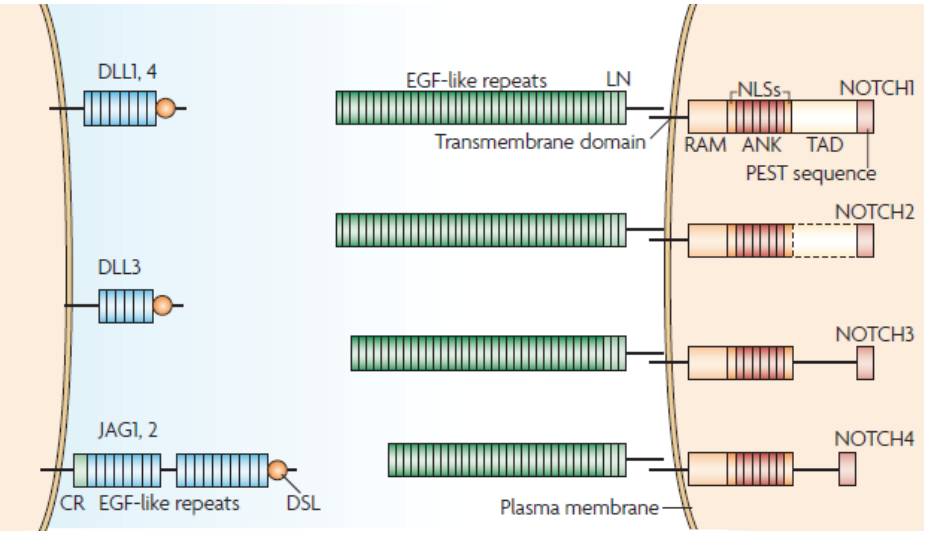

Figure 2. Molecular components of the Notch pathway. The five ligands share structural homology including a DSL domain, a variable number (6-18) of EGF-like repeats, a transmembrane domain and a small cytoplasmic tail. JAG1 and JAG2 have also a cysteine-rich domain. The four receptors also share structural homology, with EGF-like repeats, LNR domain, a juxtamembrane region with specific proteinase cleavage sites, a transmembrane region including a cleavage site for γ-secretase, and a cytoplasmic region that contains several functional domains (RAM, ANK, NLS,TAD and PEST described in the text). TAD domain is weaker in NOTCH2 compared to NOTCH1 while it is absent in NOTCH3 and NOTCH4 [DLL: Delta-like ligand; JAG: Jagged; DSL: Delta, Serrate and LAG2; CR: cysteine-rich domain]. (Thurston et al., 2007).

Canonical Notch activation is initiated when receptors engage ligands expressed on a neighboring cell. Ligand binding to repeats within the EGF-like domain of the receptor causes two sequential proteolytic events called S2 and S3 cleavages, mediated by ADAM (a disintegrin and metalloproteinase family) or TACE (TNF-α converting enzyme) and by γ-secretase, respectively. Ligand binding causes the exposure of the S2 cleavage site otherwise buried within the NRR in the "off-state" of the receptor. The two consecutive cleavages produce the Notch intracellular domain (ICN) which is released from the plasma membrane and

moves to the nucleus. Once in the nucleus, the ICN interacts with members of the RBPJ or CSL (CBF1, Su(H) and LAG1) family of transcription factors and coactivators of the MAML (mastermind-like) family. ICN is unable to bind DNA on its own but needs CSL that directs it to specific targets. On the contrary, in absence of ICN CSL can form complexes with many co-repressor protein such as NcoR and SHARP. The nuclear complex composed by CSL/ICN/MAML recruits histone acetyltransferases, chromatin remodeling factors and mediator complex to assemble an active transcription complex on target gene promoters. (Fig. 3).

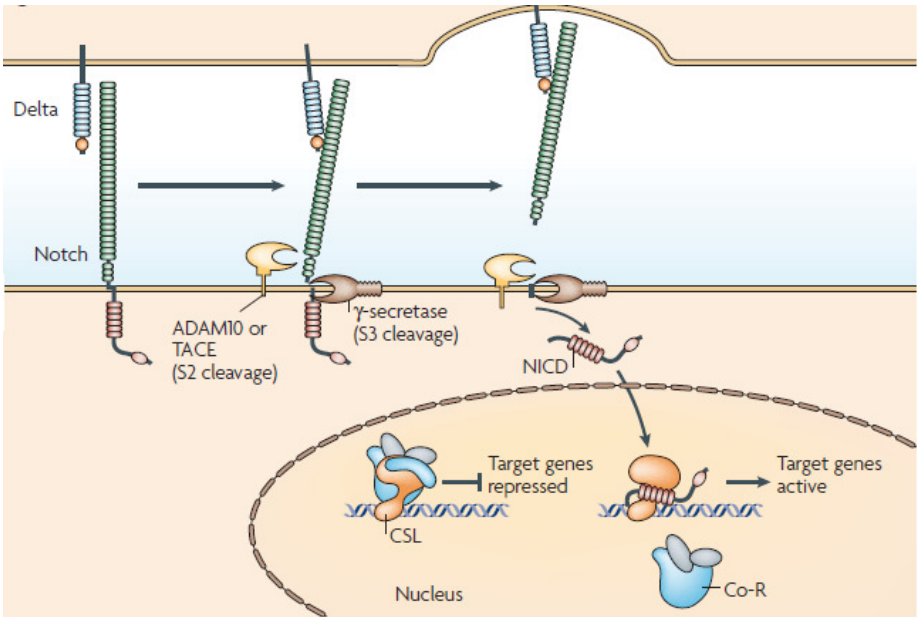

Figure 3. Mechanism of Notch signaling. After the binding to a ligand, Notch receptor undergoes two proteolytic cleavages resulting in the release of the Notch intracellular domain (ICN) which transfers to the nucleus. Here ICN interacts with the CSL family of transcription factors, leading to conversion of the transcriptional co-repressor complex into an activator complex, and thus induce the expression of target genes. [CSL family: CBF1 for humans, Suppressors of hairless for drosophila, LAG for *Caenorhabditis elegans*, RBPJ in the mouse; Co-R: co-repressor; TACE: TNF-α converting enzyme, also known as ADAM17; NICD: Notch intracellular domain] (Thurston et al., 2007).

Regulation of either ligand or receptor availability at cell surface is very important to control Notch activation because each Notch molecule that undergoes proteolysis generates a signal and thus can only signal once. For this reason,

frequently ligand and/or receptor expression is spatially and temporally restricted. Moreover, ligands and receptors can be subjected to regulation by other signaling pathway and can have overlapping as well as distinct expression patterns during development. The outcome of Notch activation depends on cellular context and dose, it varies from differentiation to maintenance of stemness, apoptosis to cell survival, uncontrolled growth to growth arrest. (Aster and Blacklow, 2012; Kopan and Ilagan, 2009; Sanchez-Irizarry et al., 2004) .

Among Notch target genes, very important are the helix-loop-helix transcription factor of the *HES* (Hairy Enhancer of Split) family such as *HES1* and the *HERP* (Hes-Related repressor protein) transcription factor family. Also *NRARP* (notch-regulated ankyrin repeat-containing protein), *NFκB*, *DELTEX-1*, *NOTCH3*, *PTCRA* (pre-TCRα or pTα) are Notch target genes (Radtke et al., 2004). Furthermore, Notch pathway directly controls key regulators of cell proliferation and metabolism such as *p27Kip1*, *mTOR* and *c-MYC* (Chan et al., 2007; Dohda et al., 2007; Palomero et al., 2006; Sharma et al., 2006; Weng et al., 2006).

Sustained Notch activation can be deleterious, so cells must regulate ICN production and the duration of signaling. In most cells signal strength is regulated by ensuring that ICN half-life is short, indeed during the transcriptional activation process ICN is phosphorylated on its PEST domain and targeted for proteasomal degradation by the E3 ubiquitin ligase FBW7. This process eliminates ICN, disassembles the ternary complex and resets the cell for the next round of signaling.

There are different modulators that regulate Notch signaling both at extracellular, cytoplasmic and nuclear levels. One possible modulation is fucose addition to specific residues within the EGF-like domain of Notch receptors, this can be further modified by the addition of N-acetylglucosamine mediated by Fringe proteins, a family of glycosyltransferase. This modification inhibits Jagged1-mediated Notch1 signaling and potentiates Delta-mediated signaling. It remains to be determined whether glycosylation regulates the adhesion strength between Notch and its ligands. Among cytoplasmic modulators, there are Deltex1 and the

negative regulator Numb, which prevents nuclear translocation of ICN and so suppresses Notch signaling. Nrarp and Mint (Msx2-interacting nuclear target protein in mouse, SHARP in humans) are nuclear regulators of Notch activity: Nrarp interacts with ICN and CSL inhibiting Notch1 signaling and moreover is a Notch target gene, Mint is also a negative regulator because competes with ICN for binding to CSL (Radtke et al., 2004).

1.2.2 Notch signaling and pathogenesis of T-ALL

The first hint that Notch signaling could be important for T cell development was in 1991, when a chromosome translocation (7;9)(q34;q34.3) involving Notch1 gene was discovered in patients with T-ALL (Ellisen et al., 1991). Several experiments and gain-of-function or loss-of-function genetic models have later confirmed the key role of Notch for T cell differentiation. The Notch-related oncogenic activity is almost exclusively restricted to T progenitors, suggesting a special developmental role for Notch in this lineage. Notch1 receptor, indeed, has a critical role in committing lymphoid precursors to the T versus B cell fate and Notch1-deficient mice lack T cell committed precursors in the thymus and contain increased numbers of early B cell precursors and mature B cells (Wilson et al., 2001). Since Notch drives T cell development, in the bone marrow stem cell niche Notch signaling must be kept below a certain threshold, so prior to ETP stage Notch signaling level is very low. Notch signaling initiates in the early T cell precursors and increases as cells mature toward the DN3 stage of development. In the DN3 stage, T cell pass through a critical checkpoint - the β-selection - that requires both the signal generated by the pre-TCR and Notch1 signaling. DN3 cells that receive both signals proliferate rapidly, on the contrary cells that don't receive signals undergo apoptosis. Beyond β-selection, Notch signaling and *NOTCH1* expression are down-regulated by mechanisms poorly understood and cell division finishes. *NOTCH1* expression strongly correlate with the expression of *c-MYC*, which is a target of Notch required for the proliferative burst that accompanies β-selection. Down-regulation of *NOTCH1* and *c-MYC* that takes

place after β-selection probably serves to limit the duration and extent of normal thymocyte proliferation. As a consequence, failure to down-regulate Notch1 signaling may be an important feature of T-ALL pathogenesis because continued expression of *NOTCH1* may block differentiation, allow the survival of cells that would normally be deleted and the expansion of cells. (Fig. 4) (Aster et al., 2008).

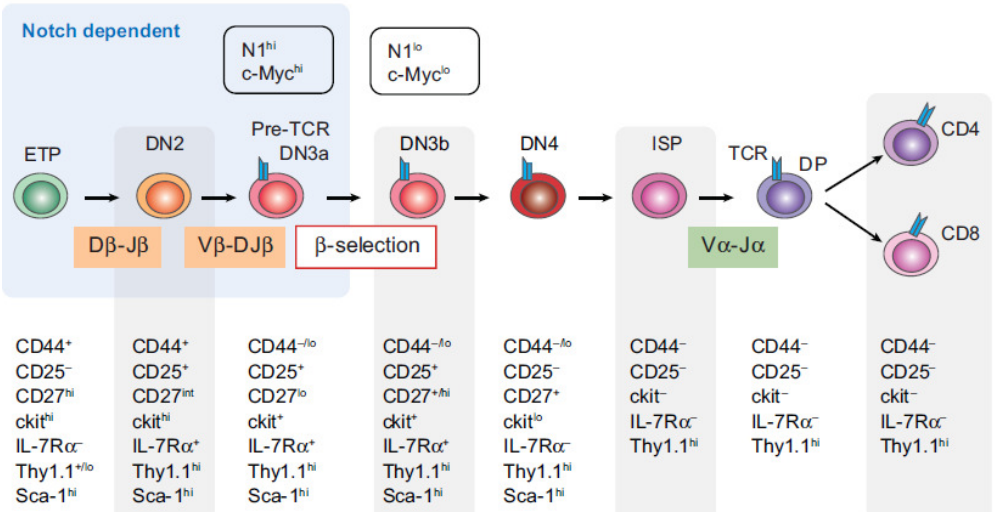

Figure 4: Notch1 and T cell development. Different stages of T cell development, characterized by immunophenotypic features shown below each stage. Notch1 is required during maturation to the DN3a stage and its expression is down-regulated, together with *c-MYC* expression, after β selection [DN, CD4−/CD8− double negative; ISP, intermediate single positive; DP, CD4+/CD8+ double positive; TCR, T cell receptor] (Aster et al., 2008).

In addition of these functions, Notch1 interacts with other genes implicated in the regulation of T cell development, such as *IKAROS*, *E2A* and *NFκB*. Ikaros is a transcriptional regulator critical for the development of all lymphoid-derived cells, which can be expressed in multiple isoforms with different DNA-binding activities. Beverly and Capobianco (Beverly and Capobianco, 2003) demonstrated that Notch and Ikaros cooperate in leukemogenesis. They found that Ikaros can bind the same regulatory elements as the Notch effector CSL, thus blocking the ICN-mediated activation of the reporter, and that the dominant negative Ikaros isoform may enhance CSL binding to enhancer/promoter elements. Combinations

of mutations that lead to loss of Ikaros transcriptional repression and gain Notch activity have been found even in other models (Dumortier et al., 2006; Lopez-Nieva et al., 2004). E2A is a basic helix-loop-helix transcription factor required for normal lymphoid development and acts together with Notch signaling to initiate T-lineage specification. They interact at different levels, since E2A induces the expression of genes involved in Notch signaling - including *HES1*, *NOTCH3*, *NOTCH1*- and moreover E2A acts in concert with Notch signaling to induce *pTα* expression (Ikawa et al., 2006).

Finally, there is also evidence of a complex interplay between Notch and NFκB signaling in transformed T cell progenitors. It has been recently demonstrated by Espinosa and colleagues that the Notch target gene *HES1* represses the deubiquitinase CYLD, a negative regulator of IKK complex, thus sustaining NFκB activation. Moreover, they showed that the Notch-HES1-CYLD-IKK axis plays a critical role in the maintenance of T-ALL (Espinosa et al., 2010).

The key role of Notch pathway in T cell development and in leukemia pathogenesis was discovered thanks to the identification of (7;9) translocation in patients with T-ALL. However this translocation is rare therefore it cannot account for pathogenesis of most T-ALL cases. In 2004 the scenario became clearer with the discovery that more than 50% of T-ALL cases present gain-of-function mutations in *NOTCH1* gene (Weng et al., 2004). Weng and colleagues identify mutations in the heterodimerization (HD) and PEST domain of Notch1 in most Notch-dependent T-ALL cell lines and in about 55% of primary T-ALLs. The most frequent *NOTCH1* mutations (40-45% of tumors) are reported in the HD domain and they are generally single amino acid substitutions, short insertions or deletions that maintain the reading frame. As explained in the previous section, HD is the region designate to prevent inappropriate or premature activation of Notch receptors because in the off state the LNRs prevent access of metalloproteases to the S2 site by wrapping around the HD and occluding the S2 cleavage site. In the heterodimerization domain two types of mutation can be found. The most common type I consists of substitutions at conserved residues or short in-frame insertions or deletions that destabilize the heterodimer stability.

Mutations of type II, relatively rare, are tandem insertions that result in the duplication of the S2 cleavage site. Both types of mutations render Notch1 susceptible to ligand-independent cleavage at S2 site. PEST mutations are detected in 20-30% of tumors and consist of point mutations that introduce stop codons, insertions or deletions that cause a shift in the reading frame. PEST domain has an important role in regulating ICN1 turnover so mutations in this region may stabilize the intracellular Notch1 protein, owing to inhibition of FBW7-mediated degradation. FBW7 is an E3 ubiquitin ligase that forms part of the SCF complex that target ICN and other important cell cycle regulators including cyclin E and c-MYC. Interestingly, *FBW7* inactivating mutations are reported in about 8-16% of T-ALL patients and frequently they are associated to *NOTCH1* mutations, suggesting a synergistic pathogenetic effect. When mutated, FBW7 fails to bind target proteins or to tag them for degradation, in both cases prolonging their half-life (Kraszewska et al., 2012b; O'Neil et al., 2007). Different data suggest that there is a selective pressure for ever-increasing levels of Notch1 activation during progression of human T-ALL so mutations in different domains are common. Mutations in both HD and PEST domains are indeed found in 10-20% of primary T-ALLs and in most Notch-dependent cell lines (Fig. 5). *NOTCH1* mutations in T-ALL are generally heterozygous and cells continue to co-express the other wild-type *NOTCH1* allele.

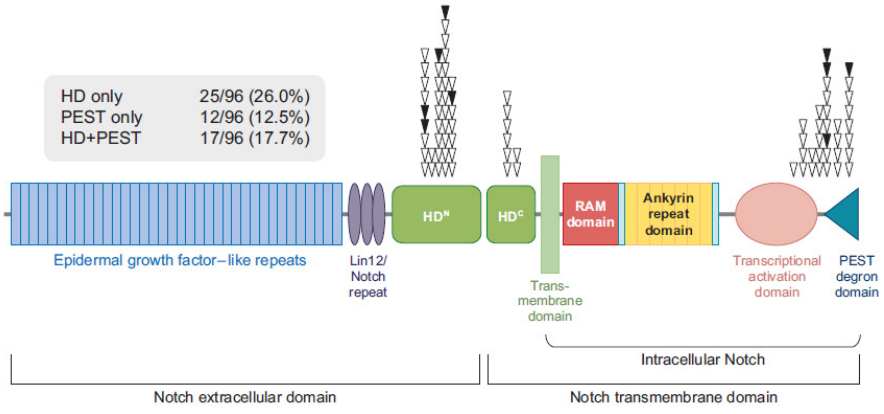

Figure 5: Distribution of Notch1 mutations in T-ALL. Each triangle stands for a mutation found in cell lines (black triangle) or primary T-ALL samples (white triangle).[HD^N and HD^C, N- and C-terminal portions of the heterodimerization] (Aster et al., 2008).

After discovery of Notch1 as a key T-ALL oncogene, one of the first issues was identification of signaling pathways and target genes regulated by Notch1. As seen before, one direct transcriptional target of ICN1 is the transcription factor *c-MYC*. c-MYC has a central role in regulating many aspects of cellular metabolism integral to the growth of cells so it is not surprising that Notch withdrawal causes downregulation of genes involved in protein synthesis, ribosome biogenesis and anabolic metabolism. Different recent papers highlight the existence of an important Notch1/c-MYC signaling axis in T-ALL cells, a feed-forward loop through which Notch1 and c-MYC reinforce the expression of genes required for the growth of T-ALL cells (Palomero et al., 2006; Sharma et al., 2006; Weng et al., 2006). Another link between Notch1 and growth pathways is represented by mTOR (mammalian target of rapamycin), key regulator of cell size and target of Notch (Chan et al., 2007).

1.2.3 Notch signaling and other malignancies

Since Notch pathway regulates many aspect of metazoan development and tissue renewal, misregulation or loss of Notch signaling are associated to multiple human disorders from developmental syndromes to adult onset diseases and cancer (Kopan and Ilagan, 2009). Regarding cancer, Notch signaling can be either oncogenic or tumor suppressive depending on the cellular context. Therefore it is not surprising that divergent context-dependent roles for Notch have emerged in cancer.

In addition to the well-known role of Notch1 in T-ALL, recent studies uncovered an oncogenic function of Notch in other hematological malignancies. Several reports suggested a role for Notch signaling in chronic lymphocytic leukemia (CLL) but the genetic evidence arrived only in 2009, when the first *NOTCH1* mutations in CLL cells were reported, and was confirmed later by different studies. A mutation in exon 34 leading to PEST degron deletion was recovered in about 5-12% of CLL cases analyzed (Di Ianni et al., 2009; Fabbri et al., 2011; Puente et al., 2011). Moreover, gain-of-function mutations were detected in

approximately 12% of mantle cell lymphoma (MCL), an aggressive neoplasm derived from naïve mature B cells (Kridel et al., 2012). Most of the reported mutations lead to PEST degron deletions as observed in CLL. Interestingly, *NOTCH1* mutations in CLL and MCL differ from those in T-ALL. Almost all of the mutations are PEST deletions and the majority (90% in CLL and >50% in MCL) consist of a deletion of the same 2 nucleotides in a codon. On the contrary, in T-ALL most frequent mutations are in the HD region and PEST mutations occur across a wide region, although the most common *NOTCH1* mutation in PEST domain is the same deletion of two nucleotides as CLL and MCL. Beyond MCL, two groups identified mutations in *NOTCH1* (Fabbri et al., 2011) or *NOTCH2* (Lee et al., 2009) PEST domains in diffuse large B cell lymphoma. These findings suggest that Notch may have additional uncharacterized roles in the development or function of B cells (South et al., 2012).

With regard to solid tumors, in the last years many studies showed a role of Notch pathway in the colorectal cancer (CRC) tumorigenesis. Notch1 activity is increased in CRC as a result of β-catenin-mediated upregulation of the ligand Jagged-1 (Rodilla et al., 2009), suggesting a cooperation between WNT and Notch pathways. Furthermore *NOTCH1* is overexpressed in CRC and its expression correlates with the pathologic grade, progression and metastasis (Zhang et al., 2010). Beyond Notch1, also Notch3 has an oncogenic role in CRC since it is upregulated in metastatic samples and modulates the tumorigenic properties of CRC cells (Serafin et al., 2011). In invasive breast carcinoma overexpression of Notch1 and Jagged1 are associated to high grade tumors and poor prognosis (Reedijk et al., 2005) and aberrant Notch transcripts have been identified in breast carcinoma cell lines and primary tumors due to rearrangements of *NOTCH1* or *NOTCH2* genes (Robinson et al., 2011). Finally, enhanced expression and/or activity of Notch1 has been reported in tumor samples of patients with renal cancer (Bin Hafeez et al., 2009; Sjolund et al., 2008), prostate cancer (Bin Hafeez et al., 2009) and melanoma (Balint et al., 2005).

Many genetic evidences emerging in the past years indicate a tumor suppressor role of Notch pathway in multiple types of human squamous cell carcinoma

(SCC), although the mechanisms remain to be defined. Different loss-of-function mutations in Notch1 indeed have been reported in cutaneous, head-neck and lung SCC (South et al., 2012).

1.3 THERAPIES IN T-ALL

For many years, T-ALL has been considered and treated as a single entity but now is clear that it is a very heterogeneous malignancy, with extremely different biological features that contribute to disease development and patient outcome. Among T-ALL patients, only 70-80% of children and 40% of adults reach long-term remission and the failure rate is likely due to insufficient understanding of T-ALL biology (Kraszewska et al., 2012b). Further improvements in survival will demand a better understanding of T-ALL pathogenesis, decoding mechanisms of drug resistance and development of new therapeutic strategies. Identification of molecular pathways involved in T-ALL pathogenesis will uncover new genes whose protein products are suitable candidates for targeted therapy. For example, T-ALL patients that present the *NUP214-ABL1* fusion or amplification of *ABL1* gene may take advantage of the use of imatinib or second-generation ABL kinase inhibitors (Pui and Evans, 2006). Recent studies have identified that the novel leukemia subtype "early T-cell precursors ALL" (ETP-ALL) displays a global transcriptional profile very similar to that of normal and myeloid leukemia hematopoietic stem cells. These findings suggest that patients with ETP-ALL may benefit from new therapies directed against the myeloid or stem cell features of this leukemia, such as high dose cytarabine or targeted therapies that inhibit cytokine receptor (Pui et al., 2012; Zhang et al., 2012).

1.3.1 Risk-based treatment assignment

Among each genetic subtype of ALL, there is quite a lot of heterogeneity due to differences in cooperating mutations in cells that undergo malignant transformation and because of variable host factors that influence drug metabolism and pharmacologic effects, such as genetic polymorphisms in genes that encodes drug-metabolizing enzyme, transporters, receptors and drug targets. Due to the disease heterogeneity, treatment must be directed according to risk

groups defined by both clinical and laboratory features in order to adapt the intensity of treatment among subsets of children with T-ALL.

The risk-based treatment assignment mainly depends on factors that can be grouped in three categories:

1. Patient characteristics. Among the most important patient features that affect prognosis there are the age at diagnosis (better prognosis for children aged 1 to 10 years compared to infants, older children and adolescent), the white blood cell count at diagnosis (WBC $5x10^4/\mu l$ is the cut-off between good and poor prognosis), central nervous system involvement at diagnosis (about 3% of patients have detectable CNS involvement with > 5 WBC/µl in the cerebrospinal fluid, it is associated to a higher risk of failure) and testicular involvement at diagnosis (it occurs in approximately 2% of male, according to some protocols it is an adverse prognostic factor).

2. Leukemic cell characteristics. Leukemic features that affect prognosis include the immunophenotype (for example ETP-ALL, subset with the poorer prognosis, is characterized by the distinctive immunophenotype $CD1a^-$ $CD8^-$ $CD5^{weak}$ with co-expression of stem cell or myeloid markers) and cytogenetics (high hyperdiploidy and hypodiploidy are positive and negative prognostic factors, respectively; *MLL* gene rearrangements are a negative prognostic factor; *ETV6-RUNX1* rearrangement is a positive prognostic marker)

3. Response to initial treatment. Since treatment response is influenced by the drug sensitivity of leukemic cells and host pharmacogenomics and pharmacodynamics, the rapidity of leukemic cells clearance following onset of treatment and the levels of residual disease at the end of the induction have a strong prognostic significance. The response to initial treatment can be evaluated in different ways. The first is the MRD (minimal residual disease) determination that can be obtained by PCR of patient specific *Ig/TCR* rearrangement or by flow cytometry, if a

leukemia-specific immunophenotype can be identified. Both techniques are specific and sensitive (detection of 1 leukemic cell in $1x10^5$ normal cells), afford levels that cannot be attained through traditional morphologic assessments (detection of 1 leukemic in 20 normal cells). In the AIEOP-BFM (Associazione Italiana Ematologia Oncologia Pediatrica- Berlin Frankfurt Münster) ALL 2000 trial the MRD status at day 78 has been proposed as the most important predictor for relapse in patients with T-ALL because MRD accounts for all the leukemic-cell biological features (including drug sensitivity), host pharmacodynamics and pharmacogenomics, and efficacy of the treatment regimen. Besides MRD determination, a good response to initial treatment can be established by reduction of leukemic cells to less than 5% in the BM within 7 or 14 days following initiation of therapy or by reduction in peripheral blast count to less than 1000/µl after steroid induction prophase. Finally leukemia cell response to treatment can be evaluated in the peripheral blood 7-10 days after the beginning of multiagent chemotherapy, patients with persistent circulating leukemic cells are at increased risk of relapse.

Different study groups stratified patients into prognostic risk groups by considering various factors among those mentioned above. The BFM (Berlin-Frankfurt-Münster) protocols base the risk stratification of pediatric patients only on treatment response criteria. In addition to prednisone response, treatment response is evaluated by MRD determination at two time points, precisely at the end of induction (week 5) and at the end of consolidation phase (week 12). According to this classification patients are divided in: *Standard Risk* if they are MRD-negative at both time points analyzed, *Intermediate Risk* if they have positive MRD at week 5 and low MRD ($<10^{-3}$) at week 12 and *High Risk* if they have high MRD ($\geq 10^{-3}$) at week 12 or if they are poor responder to prednisone prophase, regardless of subsequent MRD (NCI web site, see reference).

1.3.2 Treatment of childhood T-ALL

Treatment of childhood T-ALL is based on specific protocols designed according to risk group stratification. This approach allows patients with favorable clinical and biological features, who are likely to have a very good outcome, to receive a relatively mild treatment, whereas patients with poor prognosis receive a more aggressive therapy that - albeit potentially more toxic - may eventually increase survival. Therapy of T-ALL is generally divided into three phases: remission induction therapy followed by consolidation/intensification therapy and then maintenance/continuation treatment.

The primary goal of remission induction is the eradication of more than 99% of T-ALL cells from blood and bone marrow and to restore normal hematopoiesis and a normal performance status. It is very important to completely eradicate leukemic cells also from extramedullary sites, since T-ALL often involves these sites. Although protocols for pediatric ALL consider the same classes of drugs for remission induction, there is no consensus on what constitutes an optimal regimen. Remission induction therapy usually includes a glucocorticoid, vincristine and asparaginase because they have distinct mechanisms for their antileukemic effects and may act synergistically. Prednisone has been the glucocorticoid most used but recently dexamethasone replaced it in different clinical trials because of its long half-life and excellent CNS penetration. Cytotoxic effects of these class of drugs are due to the glucocorticoid-mediated inhibition of cytokine production, alteration of oncogenes expression and induction of cell cycle arrest and apoptosis (Inaba and Pui, 2010). In some protocols, patients are treated also with an anthracycline such as doxorubicin or daunorubicin. It has been tried to intensify induction therapy in order to reduce leukemia burden and prevent drug resistance, but intensive induction therapy led to increased morbidity and mortality.

Once remission has been achieved and normal hematopoiesis is restored, patients undergo consolidation/intensification therapy. The intensity of chemotherapy varies considerably depending on risk group assignment and, such as remission

induction, also for the consolidation/intensification therapy there is no consensus on the best regimens and their duration. This phase of treatment can be based on intermediate-dose or high-dose methotrexate, drugs similar to those used in the first phase (asparaginase, vincristine, dexamethasone, with or without anthracycline), different drug combinations with little known cross-resistance to the induction therapy drugs, including cyclophosphamide, cytarabine and thiopurine or combinations of the above.

Finally, patients are subjected to maintenance/continuation treatment in order to eliminate residual leukemia cells. Patients with ALL require prolonged continuation therapy, at least two years, and attempts to shorten this phase have entailed poor results both in children and adults. The maintenance/continuation therapy is based on the combination of methotrexate and mercaptopurine administrated weekly and daily respectively, with or without pulses of dexamethasone and vincristine (Pui and Evans, 2006; Pui et al., 2012). In some protocols boys are treated longer than girls because prognosis for girls is slightly better for reasons that are not well understood (NCI web site).

As mentioned before, in approximately 3% of T-ALL patients there is a detectable CNS involvement at diagnosis, with ≥5 WBC/μl recovered in the cerebrospinal fluid. Potentially the majority of children will develop overt CNS leukemia therefore all pediatric patients should receive systemic combination chemotherapy together with CNS prophylaxis. Standard treatment options include intrathecal chemotherapy with methotrexate alone or in combination with cytarabine and hydrocortisone, CNS-penetrant systemic chemotherapy based on dexamethasone, L-asparaginase and high-dose methotrexate with leucovorin rescue and cranial radiation. Once more, the type of CNS-therapy used is based on the patient's risk group and the risk of CNS-relapse. Cranial radiation is usually directed only to the highest risk for subsequent CNS relapse, the use of cranial radiation indeed has decreased significantly in the past years especially for pediatric patients due to many late-occurring injuries such as second cancer, neurocognitive impairment and multiple endocrinopathy. In very high risk patients that still receive cranial radiation, the dose has been significantly reduced. (Pui and Evans, 2006; Pui et

al., 2012). Intrathecal chemotherapy is usually started at the beginning of induction, intensified throughout consolidation and in some protocols continued during the maintenance phase (NCI web site).

In the event of relapse, initial treatment consists in a four-drug reinduction regimen similar to that administrated to newly-diagnosed high risk patients or a therapy with high-dose methotrexate and high-dose cytarabine. Patients with refractory or multiple-relapsed leukemia are commonly treated with a combination of clofarabine, cyclophosphamide and etoposide (NCI web site).

Leukemia patients have a limited bone marrow reserve of normal hematopoietic cells therefore it can be necessary to opt for prophylactic antibiotics and antifungal agents to prevent serious infections, particularly if high-dose dexamethasone therapy is prolonged or combined with other cytotoxic chemotherapies (Inaba and Pui, 2010).

Finally several novel nucleoside analogues have revealed promising results in the treatment of T-ALL, such as clofarabine, forodesine and nelarabine. The last is the most studied, it is a soluble nucleoside analogue that is converted in the active nucleotide and then is incorporated into DNA, resulting in chain termination and cell death. The nucleotide preferentially accumulates in leukemic cells compared to normal cells. Other novel agents in the early phase of clinical testing include FLT3 inhibitors and γ-secretase inhibitors (GSI). As described before, γ-secretase is the enzyme that catalyzes the release of the ICN, the active form of Notch receptor. GSI were originally created for Alzheimer's disease, since γ-secretase is involved in its pathogenesis, and have subsequently been studied also in T-ALL. Unfortunately, first generation GSI cause severe gastrointestinal toxicity due to simultaneous blockade of all Notch receptors, which prevented their clinical application (Fielding et al., 2012; Pui and Evans, 2006).

2. AIM OF THE STUDY

T-cell acute lymphoblastic leukemia is an hematologic disease representing approximately 15% of the newly diagnosed cases of ALL in children and 25% in adults. Although therapeutic strategies have considerably improved in the last years, only 70-80% of pediatric and 40% of adult patients achieve long-term remission. Therefore it is necessary to develop and study new therapeutic approaches in order to convert these patients in curable.

Many studies focus the Notch pathway, because its role during T cell development is well established and because mutations in *NOTCH1* gene are found in about 50-55% of T-ALL cases. Previous attempts to target Notch signaling in T-ALL were mainly based on administration of GSI (gamma-secretase inhibitors), which unfortunately disclosed poor efficacy and severe gastro-intestinal toxicity due to simultaneous inhibition of Notch1 and Notch2 signaling in gut epithelial cells.

Starting from these evidences, the main purpose of the study was to investigate therapeutic efficacy of selective targeting of Notch1, which may overcome some limits of broad-spectrum therapies. To these end, we generated a clinically relevant model of T-ALL and used it to test the therapeutic and biological effects of a novel neutralizing monoclonal antibody directed against human Notch1. To investigate mechanisms involved, we analyzed effects of the therapy on cell death, proliferation and gene expression. Moreover, we identified new predictive biomarkers of response which could be helpful for clinical development of this drug and investigated possible synergistic effects of Notch1 blockade with consolidated drugs used for T-ALL patients.

3. MATERIALS AND METHODS

3.1 T-ALL xenografts establishment and tumorigenicity assay

Primary T-ALL cells (PDTALL) were obtained from bone marrow (BM) of newly diagnosed pediatric patients, according to the guidelines of the local ethics committees. For xenografts establishment, 6- to 9-weeks-old mice were injected intravenously (i.v.) with 10 x 10^6 T-ALL cells in 300 µl of Dulbecco's Phosphate Buffer Saline (PBS). NOD/SCID mice were purchased from Charles River (Wilmington, MA). Procedures involving animals and their care conformed with institutional guidelines that comply with national and international laws and policies (EEC Council Directive 86/609, OJ L 358, 12 December, 1987). T-ALL engraftment was monitored by periodic blood drawings and flow cytometric analysis of CD5 and CD7 markers over a 5-month period. To test the effect of Notch1 blockade on leukemia engraftment, NOD/SCID mice were treated with anti-human Notch1 mAb OMP-52M51 (Oncomed Pharmaceuticals Inc., Redwood, CA) or control antibody (Rituximab, Roche, Basel, Switzerland) administrated intraperitoneally (i.p, both used at 20 mg/Kg) two days after i.v. injection of T-ALL cells (5x10^6 cells/mouse). Anti-Notch1 or control antibody were subsequently administrated weekly for an average of 3 doses (6 mice/group). In the late intervention trial, administration of OMP-52M51 started 11 days after leukemia cell injection, followed by a second dose one week later. In the experiment with combination of dexamethasone and anti-Notch1, the first was administrated i.p everyday (used at 10 mg/Kg) while anti-Notch1 was administrated weekly as starting 11 days after cells injection. In all experiments, mice were inspected twice weekly to detect early signs and symptoms of leukemia and blood was drawn to measure T-ALL cell engraftment.

3.2 Cytofluorimetric analysis and cell sorting

Anti-human FITC-conjugated CD5 and PE-Cy5-conjugated CD7 antibodies (Coulter, Fullerton, CA) were used for the detection of T-ALL cells in blood,

spleen and bone marrow samples. Apoptosis and proliferation were evaluated by the Annexin-V-FLUOS Staining Kit (Roche Diagnostics, Penzberg, Germany) and the AlexaFluor 488-labeled Ki67 staining (BD Biosciences, San Jose, CA) respectively. In order to exclude murine cells from the analysis, only human $CD5^+$ cells were considered for both apoptosis and proliferation assays. Samples were analyzed on Beckman Coulter EPICS-XL Flow Cytometer (Coulter) or BD LSRII Flow Cytometer (BD Biosciences). Dot plots images were processed by Flow Jo software (TreeStar, Ashland, OR). For fluorescence glucose analysis, cells were incubated with 2-N-[(7-nitrobenz-2-oxa-1,3-diazol-4-yl)amino]-2-deoxy-D-glucose (2-NBDG) for 1 minute and analyzed at FACS without washing, considering only human $CD5^+$ cells.

T-ALL cells from bone marrow and spleen were incubated with PE-Cy5-conjugated antibody against human CD5 and sorted on a BD FACS Aria III cell sorter (BD Biosciences). Relative percentages of the $CD5^+$ subpopulation were calculated based on viable gated cells (as indicated by physical parameters, side scatter and forward scatter). After sorting, an aliquot of the sorted cells was used to check the purity of the population.

3.3 Optical imaging of tumors

To perform in vivo imaging, leukemia cells were transduced by a lentiviral vector encoding the luciferase gene. *In vivo* bioluminescence images were acquired at several time points after cells injection on IVIS Imaging System (Xenogen Corporation, Alameda, CA). Eight minutes before imaging, animals were anesthetized and injected i.p. with 150 mg/kg of D-luciferin (Biosynth AG, Staad, Switzerland) in Dulbecco's Phosphate Buffer Saline (PBS). During acquisitions animals were maintained under slight gas anesthesia (isoflurane 2%). Signal intensity was quantified as average radiance within a region of interest prescribed around the tumor sites (photons/s/cm^2) using the LivingImage® software (Xenogen).

3.4 Reverse Transcription-PCR and quantitative PCR (qPCR)

Total RNA was isolated using TRIzol® Reagent according to manufacturer's instructions. cDNA was synthesized from 1-1.5 μg of total RNA using High Capacity RNA-to-cDNA kit. For qPCR analysis, the SYBR Green dye and ABI Prism 7900 Sequence Detection System were used. Relative quantification was done using the ΔΔCt method, normalizing to β2-microglobulin mRNA. Primers used for qPCR analysis are: CR2-for: 5'-CTGCGGTTCAGTGTCCACAT-3'; CR2-rev: 5'-GGTGAAGCCAAACATGCAAGC-3' ; DTX-1-for: 5'-GTGGGCTGATGCCTGTGAAT-3'; DTX-1-rev: 5'-CGAGCGTCCTCCTTCAGCAC-3'; HES1-for: 5'-GGCGGCTAAGGTGTTTGGAG-3'; HES-1 rev: 5'-GGAAGGTGACACTGCGTTGG-3'; NOTCH3-for: 5'-CAAGGGTGAGAGCCTGATGG-3'; NOTCH3-rev: 5'-GAGTCCACTGACGGCAATCC-3'; pTa-for: 5'-ATGGTGGTGGTCTGCCTGGT-3'; pTa-rev: 5'-AGTTGGTCCAGGTGCCATCC-3'; β2-microglobulin-for 5'-TGCTGTCTCCATGTTTGATGTATCT-3'; β2-microglobulin-rev: 5'-TCTCTGCTCCCCACCTCTAAGT-3'.

For analysis of the Notch pathway activation, 21 Notch target genes (see list below in Table I) were evaluated in duplicates by Custom TaqMan®Array Cards using TaqMan® Universal PCR Master Mix and ABI Prism 7900 Sequence Detection System. Relative quantification was done using the ΔΔCt method, normalizing to β2-microglobulin mRNA. All reagents were obtained from Life Technologies, Paisley, UK.

Gene	Assay ID	Description
B2M	B2M-Hs99999907_m1	beta-2-microglobulin
p27	CDKN1B-Hs00153277_m1	cyclin-dependent kinase inhibitor 1B (p27, Kip1)
p18	CDKN2C-Hs00176227_m1	cyclin-dependent kinase inhibitor 2C (p18, inhibits CDK4)
CR2	CR2-Hs00153398_m1	complement component (3d/Epstein Barr virus) receptor 2
DTX1	DTX1-Hs00269995_m1	deltex homolog 1 (Drosophila)
GAPDH	GAPDH-Hs99999905_m1	glyceraldehyde-3-phosphate dehydrogenase
GIMAP5	GIMAP5-Hs00218095_m1	GTPase, IMAP family member 5
HES1	HES1-Hs00172878_m1	hairy and enhancer of split 1, (Drosophila)
HES4	HES4-Hs00368353_g1	hairy and enhancer of split 4 (Drosophila)
HMBS	HMBS-Hs00609293_g1	hydroxymethylbilane synthase
LZTFL1	LZTFL1-Hs00220450_m1	leucine zipper transcription factor-like 1
MYC	MYC-Hs99999003_m1	v-myc myelocytomatosis viral oncogene homolog (avian)
NOTCH3	NOTCH3-Hs00166432_m1	Notch homolog 3 (Drosophila)
PCGF5	PCGF5-Hs00737074_m1	polycomb group ring finger 5
PGK1	PGK1-Hs99999906_m1	phosphoglycerate kinase 1
PRMT1	PRMT1-Hs00266002_m1	protein arginine methyltransferase 1
pTa	PTCRA-Hs00300125_m1	pre T-cell antigen receptor alpha
PTPRC	PTPRC-Hs00174541_m1	protein tyrosine phosphatase, receptor type, C
RHOU	RHOU-Hs00221873_m1	ras homolog gene family, member U
RPL10A	RPL10A-Hs01912344_uH	ribosomal protein L10a
SHQ1	SHQ1-Hs00250772_m1	SHQ1 homolog (S. cerevisiae)
SKP2	SKP2-Hs00180634_m1	S-phase kinase-associated protein 2 (p45)
TASP1	TASP1-Hs00214554_m1	taspase, threonine aspartase, 1
ZAP70	ZAP70-Hs00277148_m1	zeta-chain (TCR) associated protein kinase 70kDa

Table I: List of the 21 Notch target genes analyzed in Custom TaqMan®Array Cards.

3.5 *NOTCH1* and *FBW7* mutational analysis

Genomic DNA was extracted from T-ALL cells derived from xenografts with Easy DNA kit (Life Technologies). *NOTCH1* and *FBW7* mutation analysis was performed as describe in (Sulis et al., 2008; Thompson et al., 2007) in collaboration with Prof. Adolfo Ferrando (Dept. of Pediatrics, Columbia University Medical Center, New York, USA).

3.6 Clonality analysis of *TCR* genes in T-ALL cells

PCR analysis to detect *TCRD*, *TCRG* and *TCRB* rearrangements was performed using methods published elsewhere (van Dongen et al., 2003; van Dongen et al.,

1999). *TCR* gene rearrangements were analyzed in the primary leukemia cells at diagnosis and in the cells obtained from xenografts, in order to check if clonality was maintained after passage into NOD/SCID mice. Clonal gene rearrangements, identified by homo/heteroduplex analysis, were sequenced by dye-terminator cycle sequencing kit on ABI Prism 310 (Life Technologies) (Germano et al., 2001) in collaboration with Prof. Giuseppe Basso's lab (Lab. Oncoematologia, Dip. di Salute della Donna e del Bambino, Università di Padova).

3.7 Preparation of cRNA, GeneChip microarray analysis and data normalization

Total RNA was isolated using TRIzol® Reagent (Life Technologies) according to manufacturer's instructions. Sense-strand cDNA from total RNA was prepared using the Ambion® WT Expression Kit (Life Technologies, Paisley, UK). The cDNA was then fragmented and labeled using the Affymetrix GeneChip ® WT Terminal Labeling kit (Affymetrix, Santa Clara, CA) .Total RNA and cRNA quality was controlled by Agilent RNA 6000 Nano Kit and Agilent 2100 Bioanalyzer (Agilent Technologies, Santa Clara, CA). cDNA was quantified by ND-1000 Spectrophotometer (NanoDrop Technologies, Wilmington, DE). Labeled sense-strand cDNA was used for screening of GeneChip Human Exon 1.0 ST Array (Affymetrix). Three independent experiments were performed. Each biological replicate consisted of T-ALL cells from the bone marrow of different mice that were pooled before sorting and RNA extraction (n=3-6 samples per pool). Hybridization and scanning was conducted on the Affymetrix platform.

Based on assessment of RNA quality and on quality control analyses (including MAplots, boxplots and post-normalization hierarchical clustering), two anti-Notch 1 (aN1) and three control Ab (ctrl-Ab) treated samples were deemed suitable for data analysis. Bioinformatics and statistical analyses were performed in R (http://www.r-project.org) and Bioconductor version 2.10 (Gentleman et al., 2004). We processed core-probe-level signal using robust multi average (RMA) to generate quantile-normalized gene-level signal estimates. Affymetrix controls and

probesets that were not mapping known genes were excluded from further analysis. Two independent filters, based on overall variance and overall mean criteria, were applied to remove the probesets falling in the lowest quartile of mean expression and variance, respectively. Differential expression analysis was performed by linear model, moderating the t-statistics by empirical Bayes shrinkage, using the limma package (Smyth, 2004). The Benjamini-Hochberg false discovery rate (BH FDR) procedure was applied to correct for multiple testing and differentially expressed genes between aN1 and ctrl Ab were selected using a BH-adjusted $p< 0.05$ and absolute fold-change>1.5 as cutoff.

3.8 Gene Set Enrichment Analysis (GSEA)

We performed GSEA (Subramanian et al., 2005) to evaluate functional significance of curated sets of genes. Genes were ranked by decreasing moderated t-statistics and GSEA pre-ranked was run with default parameters. We tested the significance of gene sets in the "c2.all" collection from the Molecular Signatures Database v3.0 (http://www.broadinstitute.org/gsea/msigdb/index.jsp), consisting of 3272 gene sets corresponding to biological pathways, gene signatures published in PubMed, and genes sets curated by domain experts, including the MYC Target Gene Database.

3.9 Animal PET studies

Tumor bearing mice were investigated using a YAP-(S)-PET II (ISE srl, Pisa, Italy) small animal scanner. [^{18}F]FDG was injected with a radiochemical purity greater than 99%. and animals (n=5 per group) were evaluated when control mice developed signs of illness (15 days after T-ALL cell injection). [^{18}F]FDG PET studies were performed as follows: animals were injected in a tail vein with 4.28 ± 0.24 MBq of the tracer and images were acquired 60 minutes after tracer injection for 30 minutes. During acquisitions animals were maintained under slight gas anesthesia (isoflurane 2%). PET studies were acquired in three dimensional mode and all images were reconstructed by using the EM (Expectation Maximization) algorithm. Data were corrected for the physical decay of fluorine 18 (t1/2: 109.8) and transformed in absolute radioactivity concentration values (MBq/gr) after

calibration of the tomography using a standard phantom and considering tissue density equal to that of water. Quantification analysis were performed using PMOD 2.7 software. For each animal, maximal tumor to background ratios (Tmax/B) volume of radioactivity uptake (Volmetab) were measured. To this aim, PET images were thresholded as previously validated and described by Krak et al. to create masks for the automatic extraction of tracer distribution volume (Brepoels et al., 2007; Krak et al., 2005). We considered as upper threshold value the maximum value of radioactivity concentration in tumor, and as lower threshold a value calculated from the mean between the maximum uptake or and the radioactivity concentration present in surrounding region considered as background (torax muscle). This threshold method allowed to automatically extract the metabolic tumor volume (cm3), the maximum and the mean uptake of the tumor. Standardized Uptake Value (SUV) was calculated according to the formula: SUV = (tumor concentration activity / injected activity) / animal weight [g]). These experiments were done in collaboration with the Dr. Rosa Maria Moresco's lab (Nuclear Medicine Department, San Raffaele Scientific Institute; Fondazione Tecnomed, University of Milan Bicocca; IBFM-CNR, Milan, Italy)

3.10 Statistical analysis

Results were expressed as mean value ± SD. Statistical analysis of data was performed using Student's t-test or Mann-Whitney test. Differences were considered statistically significant when $P \leq 0.05$.

4. RESULTS

4.1 Establishment of a clinically relevant model of T-ALL

Xenografts were established by i.v. injection of primary T-ALL cells into NOD/SCID mice ($1x10^7$ cells/mouse). Leukemia engraftment was monitored by periodic blood drawings and flow cytometric analysis of the expression of human T cell-specific surface markers (CD5, CD7). Engraftment rate after a 5-month observation period was 52% and so far we obtained a collection of n=30 xenografts. As reported in Table II, pediatric patients from which T-ALL cells were obtained were classified according to phenotype, MRD class risk and prednisone sensitivity. T-ALL cells obtained from xenografts were periodically analyzed by molecular analysis in order to confirm that the same TCR rearrangement was found in the primary leukemia cells from patients and in the matched xenograft.

Sample ID	Age (years)	Phenotype	Risk	PGR/PPR	NOTCH1 status	FBW7 status
PDTALL6	13	T int	MR	PGR	wt	wt
PDTALL9	9	Early T	HR	(deceased)	wt	wt
PDTALL13	5	T	HR	(deceased)	wt	wt
PDTALL14	8	Int/mat	MR	PPR	wt	wt
PDTALL15	7	T	HR	PPR	wt	wt
PDTALL16	5	T mat	MR	PPR	wt	wt
PDTALL18	6	T int	MR	PPR	wt	wt
PDTALL28	12	T int	N/A	PGR	wt	N/A
PDTALL1	12	T int	SR	PGR	HD mut.	Mut.
PDTALL4	N/A	T	MR	PGR	HD mut.	Mut.
PDTALL7	5	T int	MR	PGR	HD mut.	wt
PDTALL10	10	Early T	MR	PGR	HD mut.	Mut.
PDTALL11	6	Thym	MR	PPR	HD mut.	wt
PDTALL20	11	T int	HR	PGR	HD mut.	wt
PDTALL21	9	T int	MR	PGR	HD mut.	wt
PDTALL5	2	T int	MR	PGR	PEST mut.	wt
PDTALL12	4	Early T	MR	PGR	PEST mut.	wt
PDTALL22	16	Early T	MR	PGR	PEST mut.	wt
PDTALL8	3	T int	MR	PPR	HD+PEST mut.	wt
PDTALL26	9	T int	N/A	PGR	HD+PEST mut.	N/A
PDTALL19	16	Early T	relapse	relapse PPR	HD+TAD mut.	Mut.
PDTALL27	9	Early T	N/A	PGR	HD+TAD mut.	N/A
PDTALL23	8	T mat	N/A	(deceased)	N/A	N/A
PDTALL24	4	T int	MR	PGR	N/A	N/A
PDTALL25	8	T	MR	PPR	N/A	N/A
PDTALL29	16	T	HR	PPR	N/A	N/A
PDTALL30	8	Early T	N/A	N/A	N/A	N/A
PDTALL31	14	T	N/A	N/A	N/A	N/A
PDTALL32	17	Early T	N/A	N/A	N/A	N/A
PDTALL33	6	T int	N/A	N/A	N/A	N/A

Table II: Pediatric T-ALL patients were classified for phenotype, risk (according to the MRD classification) and response to therapy. Patients age was 2-17 years. Mutational status of *NOTCH1* and *FBW7* are also reported. For PDTALL4, PDTALL6, PDTALL7 and PDTALL10 the genetic analysis was performed using DNA from patients at diagnosis, while for the others DNA from xenografts was utilized. [N/A= not available; SR= standard risk, MR= medium risk, HR= high risk; PGR= prednisone good responder, PPR= prednisone poor responder; HD= heterodimerization domain, PEST= proline-glutamic acid-serine-threonine-rich domain, TAD= C-terminal transcription activation domain]

4.2 Analysis of *NOTCH1/FBW7* mutations and Notch activity in T-ALL cells

Genomic DNA obtained from both primary T-ALL samples and xenografts was analyzed in order to identify possible mutations in *NOTCH1* or *FBW7* genes. Genetic analysis disclosed an heterogeneous *NOTCH1* and *FBW7* genetic status. Approximately 63% of PDTALL samples present at least one mutation in *NOTCH1* gene, including the hetero-dimerization domain HD (n=7), PEST domain (n=3), HD + PEST (n=2) or HD + TAD (n=2). Moreover, 21% (n=4) of the samples displayed also mutations in *FBW7* gene. These percentages are consistent with those reported in literature. Specific mutations are reported in Table II.

Expression levels of some Notch target genes including *CR2*, *DTX-1*, *HES1*, *NOTCH3* and *pTα* were measured by qRT-PCR in order to correlate the mutational status to the levels of activity of the Notch pathway. In general there was a good correlation between the *NOTCH1* and *FBW7* genetic status and the expression levels of Notch-related transcripts since mutated xenografts disclosed a higher pathway activation compared to wild type samples. Exceptions were PDTALL6 and PDTALL18, two xenografts with relatively sustained Notch signaling in the absence of *NOTCH1/FBW7* mutations, and PDTALL21, a xenograft with low Notch signaling notwithstanding an HD mutation (Fig. 6).

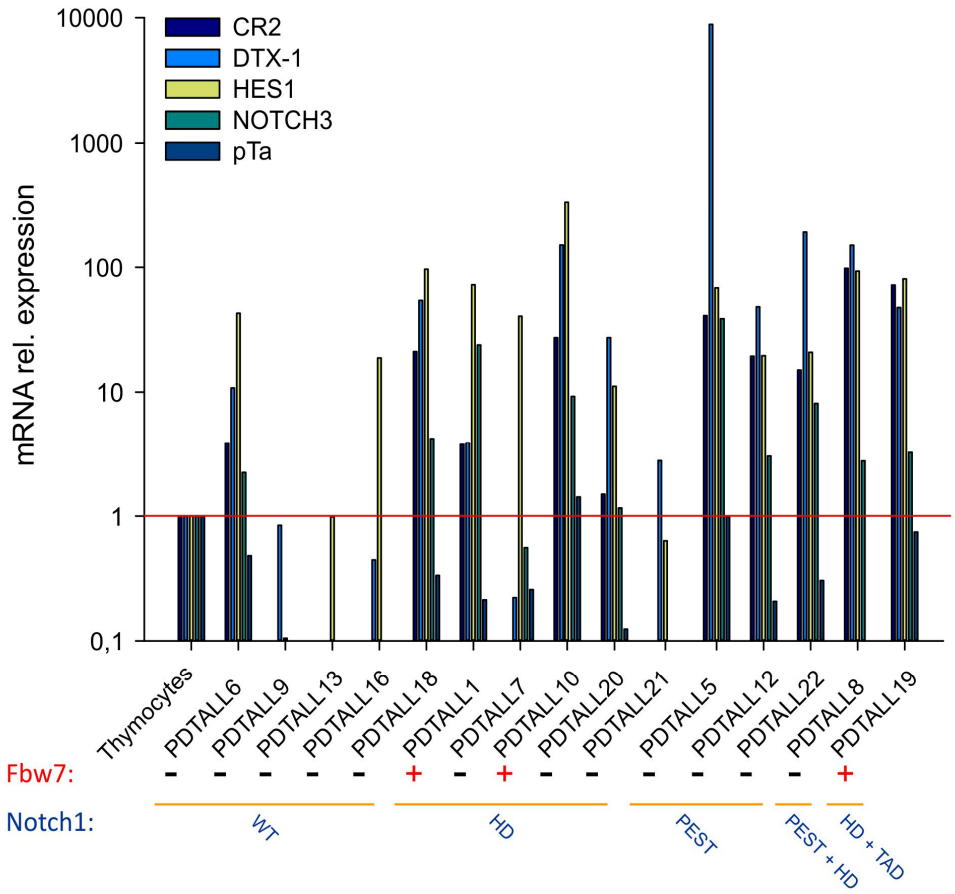

Figure 6:. Expression levels of Notch target genes in T-ALL xenografts and correlation with *NOTCH1/FBW7* genetic status. Expression levels of *CR2*, *DTX-1*, *HES1*, *NOTCH3* and *pTα* was determined by qRT-PCR and normalized to normal thymocytes (n=4 samples). The mutational status of *NOTCH1* and *FBW7* is reported below each xenograft.

4.3 Notch-blockade by receptor-specific antibody as a novel therapeutic option for T-ALL

The systemic T-ALL model thus generated was exploited to test the biological and therapeutic activity of a human Notch1-specific neutralizing antibody. OMP-52M51 was generated by immunizing mice with a fragment of human Notch1 protein consisting of the LNR plus HD domains and was selected by Oncomed Inc., among large panels of antibodies developed, due to its optimal antagonist function in ligand-dependent reporter gene assays and *in vivo* xenograft models. OMP-52M51 was indeed able to efficiently reduce Notch1 signaling driven in response to DLL4, Jag1 or Jag2 ligands in a dose-dependent way (Fig. 7, top panel) and to significantly block subcutaneous growth of HPB-ALL cells in mice (Fig. 7, bottom panel).

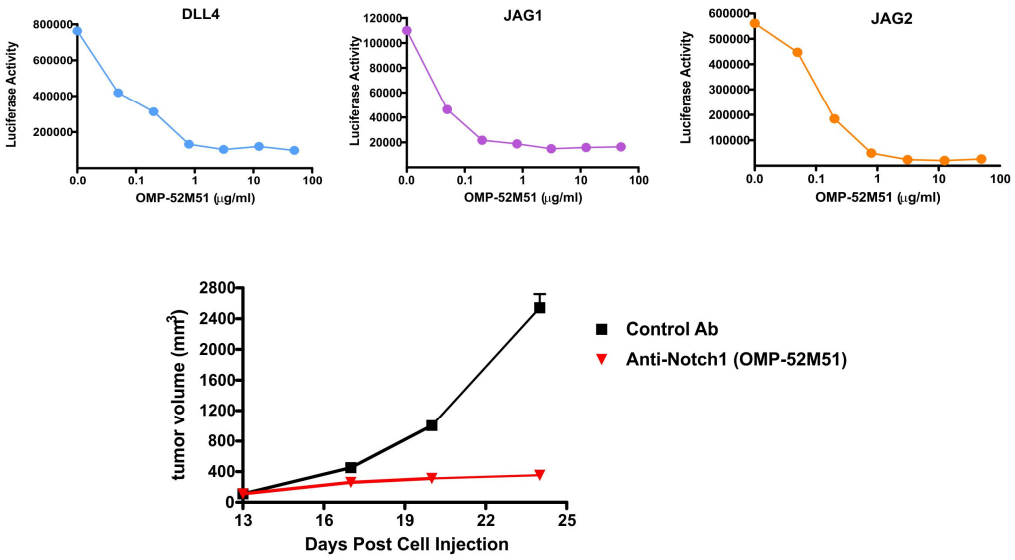

Figure 7: OMP-52M51 is an effective inhibitor of human Notch1 signaling in response to both the DLL family or the Jag family of Notch ligands. **Top:** A Notch dependent luciferase reporter gene regulated by CBF binding sites was transfected into PC-3 cells along with an expression vector encoding human Notch1. Cells were exposed to immobilized DLL4, Jag1 or Jag2 as indicated and to varying concentrations of anti-Notch1. **Bottom:** $5x10^6$ HPB-ALL cells were injected subcutaneously in NOD/SCID mice. Treatment was initiated 13 days later when tumor volumes averaged approximately 110 mm3 and continued for the duration of the experiment. Mice received either 15 mg/kg of a control antibody or OMP-52M51 twice weekly, administered by IP injection [n=10 mice per group].

In order to evaluate the efficacy of this mAb in a close-to-clinic model, we assessed its effects in n=4 xenografts bearing different *NOTCH1/FBW7* mutations and in n=3 xenografts with wild-type *NOTCH1* sequence. Initially, early intervention trials were carried out as represented in the following schematic model:

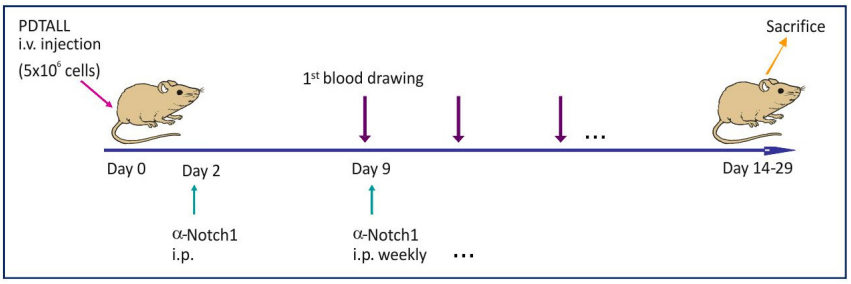

In these experiments, administration of anti-Notch1 or control antibody started 2 days after i.v. injection of T-ALL cells (6 mice/group) and tumor burden in treated compared to control mice was monitored by periodic flow cytometric analysis of blood samples for the expression of human CD5 and CD7. At the appearance of signs of illness in control mice, both groups were sacrificed and therapeutic response was evaluated by analysis of percentage of leukemic cells, levels of apoptosis and proliferation in BM and spleen.

At sacrifice, we detected significant reductions in the percentage of blasts both in the blood, in the spleen and in the BM in treated compared to control mice in PDTALL11, PDTALL12, PDTALL8 and PDTALL19. In contrast, PDTALL13, PDTALL16 and PDTALL18 were substantially resistant to Notch1 blockade. Interestingly, the therapeutic response matched the *NOTCH1/FBW7* genetic status of the T-ALL xenografts: the presence of mutations in *NOTCH1* in PDTALL11, PDTALL12, PDTALL8 and PDTALL19 xenografts correlated with good response to anti-Notch1 therapy, whereas the three xenografts with parental *NOTCH1/FBW7* sequences were poor responders.

Evaluation of $CD7^+$ cells in the three districts analyzed are reported in figure 8, furthermore these results were confirmed either by measurements of $CD5^+$ cells as additional read-out of leukemia (data not shown).

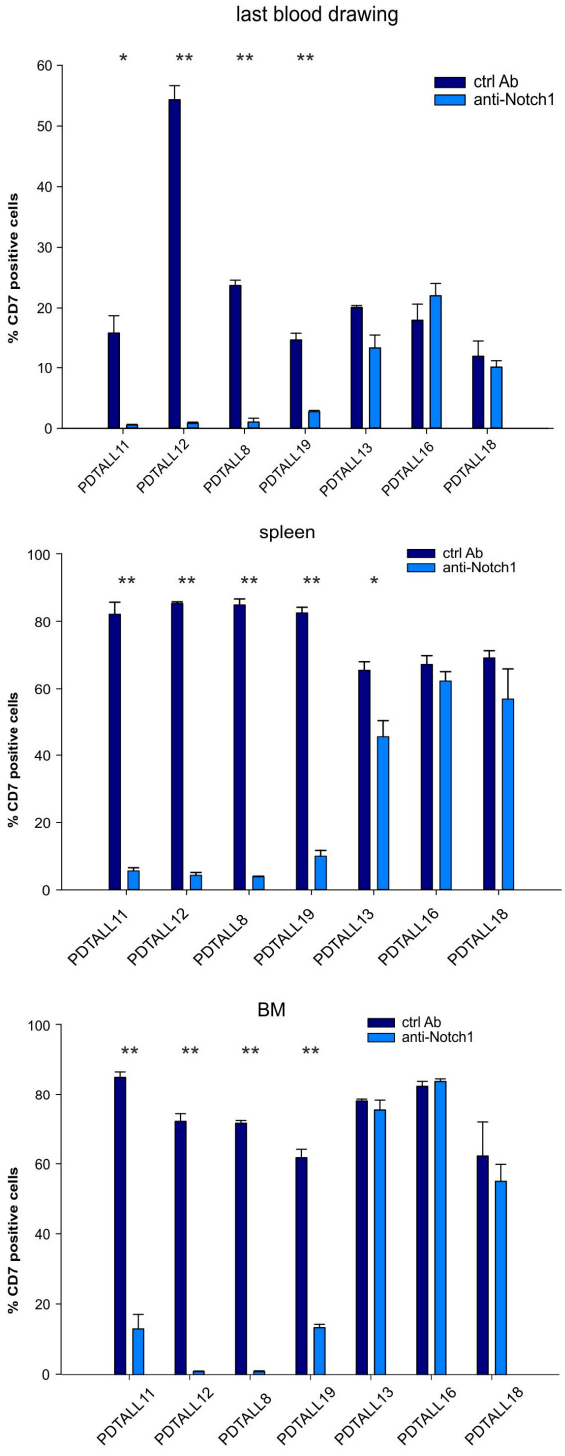

Figure 8: Anti-Notch1 inhibits growth of Notch1-driven T-ALL xenografts. **Top:** Measurement of circulating blasts by flow cytometry in the blood. **Middle:** Percentage of leukemic cells in the spleen at sacrifice. **Bottom:** Levels of T-ALL cells in the bone marrow of treated or control mice evaluated at sacrifice. Statistically significant differences in ctrl Ab versus anti-Notch1 samples are indicated (* P<0.05; ** P<0.001).

Interestingly, a clear reduction in the surface CD7 expression was measured in samples of anti-Notch1 responder xenografts (Fig. 9) but not in those poor responders. In contrast, CD5 levels were not down-modulated by treatment. The marked reduction in CD7 expression was a consistent trait following anti-Notch1 therapy and it was strictly correlated to the therapeutic response, suggesting that this parameter could be considered a candidate predictive marker.

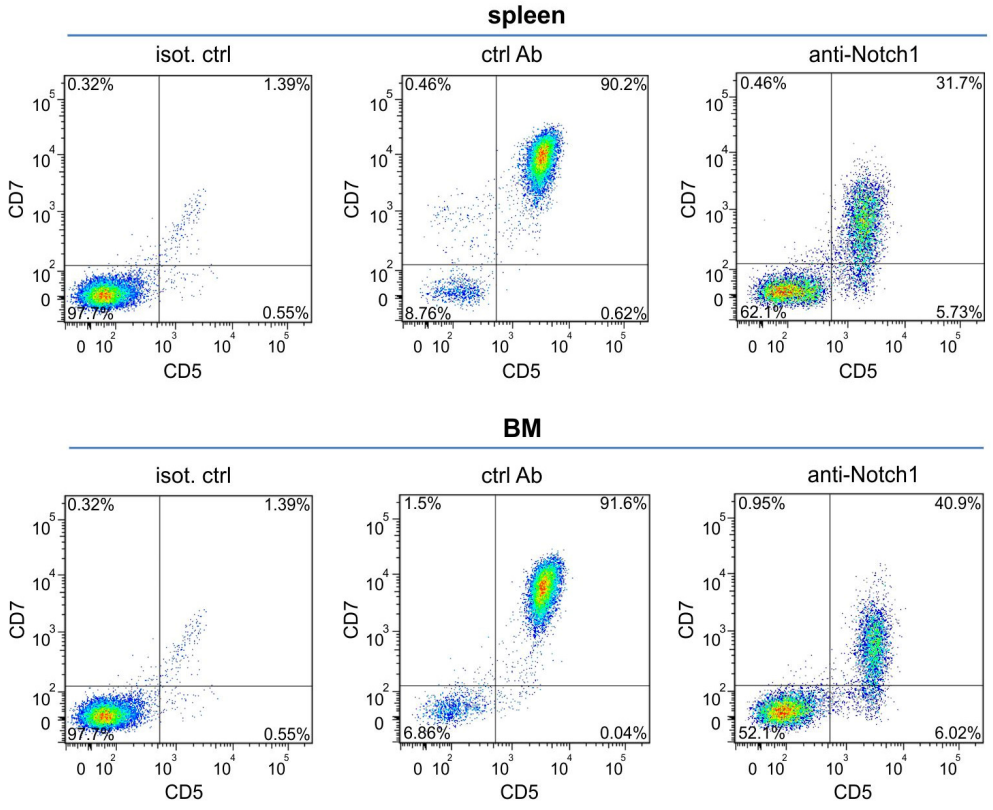

Figure 9: Representative flow cytometric analysis of CD5 and CD7 expression in spleen (**top** panel) and BM (**bottom** panel) of ctrl Ab and anti-Noch1 treated mice. This sample shows marked down-regulation of CD7 expression levels following anti-Notch1 therapy.

Furthermore, anti-Notch1 therapy was associated to an increase in the levels of apoptosis and a significant decrease of T-ALL cell proliferation both in spleen and BM (Fig. 10).

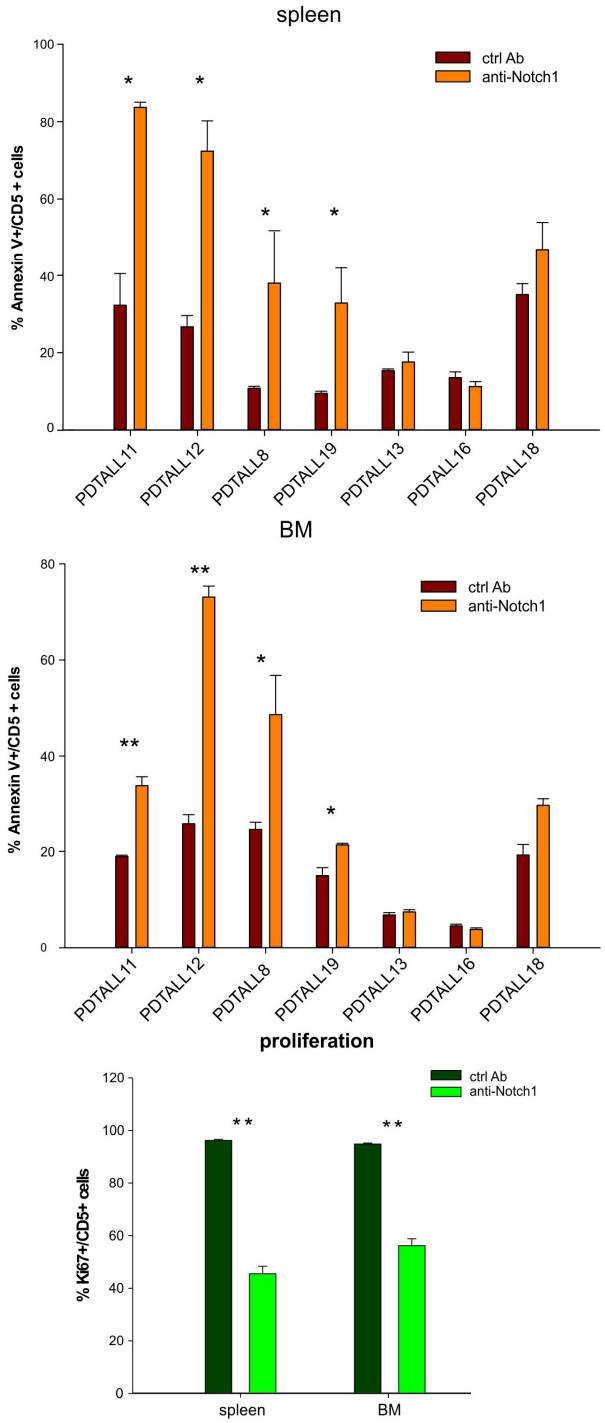

Figure 10: Effects of anti-Notch1 treatment on apoptosis and proliferation. At sacrifice, levels of apoptotic leukemic cells in the spleen (**Top** panel) and in the bone marrow (**Middle** panel) of treated or control mice were measured by annexin V labeling and flow cytometric analysis (n=6 mice/group). **Bottom** panel, evaluation of $CD5^+$ cells proliferation by Ki67 staining and flow cytometric analysis in PDTALL19 is reported (one representative experiment). Statistically significant differences in the two groups of samples are indicated (*P<0.05, **P<0.001)

In one xenograft (PDTALL19) the effect of anti-Notch1 therapy was monitored by imaging following labeling of T-ALL cells with a luciferase-expressing lentiviral vector. Optical imaging confirmed the reduction in the tumor engraftment after anti-Notch1 administration at various time points of analysis (Fig. 11, top panel). It should be noted that at day 17 anti-Notch1-treated mice lacked detectable signals while leukemia was widespread in control mice, in particular involving the spleens and the femurs.

In support of these findings, effects of anti-Notch1 treatment were detected also by [^{18}F]FDG PET imaging. These studies disclosed that [^{18}F]FDG uptake was very high in PDTALL19 xenografts receiving the control antibody, particularly in the spleen, whereas it was markedly reduced following anti-Notch1 therapy. Indeed, PET images of anti-Notch1-treated mice were very similar to those of healthy mice (Fig. 11, middle panel). This result may either reflect decreased tumor burden as shown by other techniques or it could be explained by a metabolic changes, as highlighted by GEP analysis and 2-NBDG uptake reported hereafter.

In figure 11 (bottom panel), macroscopic differences between spleens and femurs in ctrl Ab- and anti-Notch1-treated mice are shown. Splenomegaly was completely absent in anti-Notch1-treated mice. Moreover, femurs of treated animal had a reddish appearance contrasting with the pale femurs of control mice, which reflected massive infiltration and replacement of normal hematopoiesis by leukemia cells.

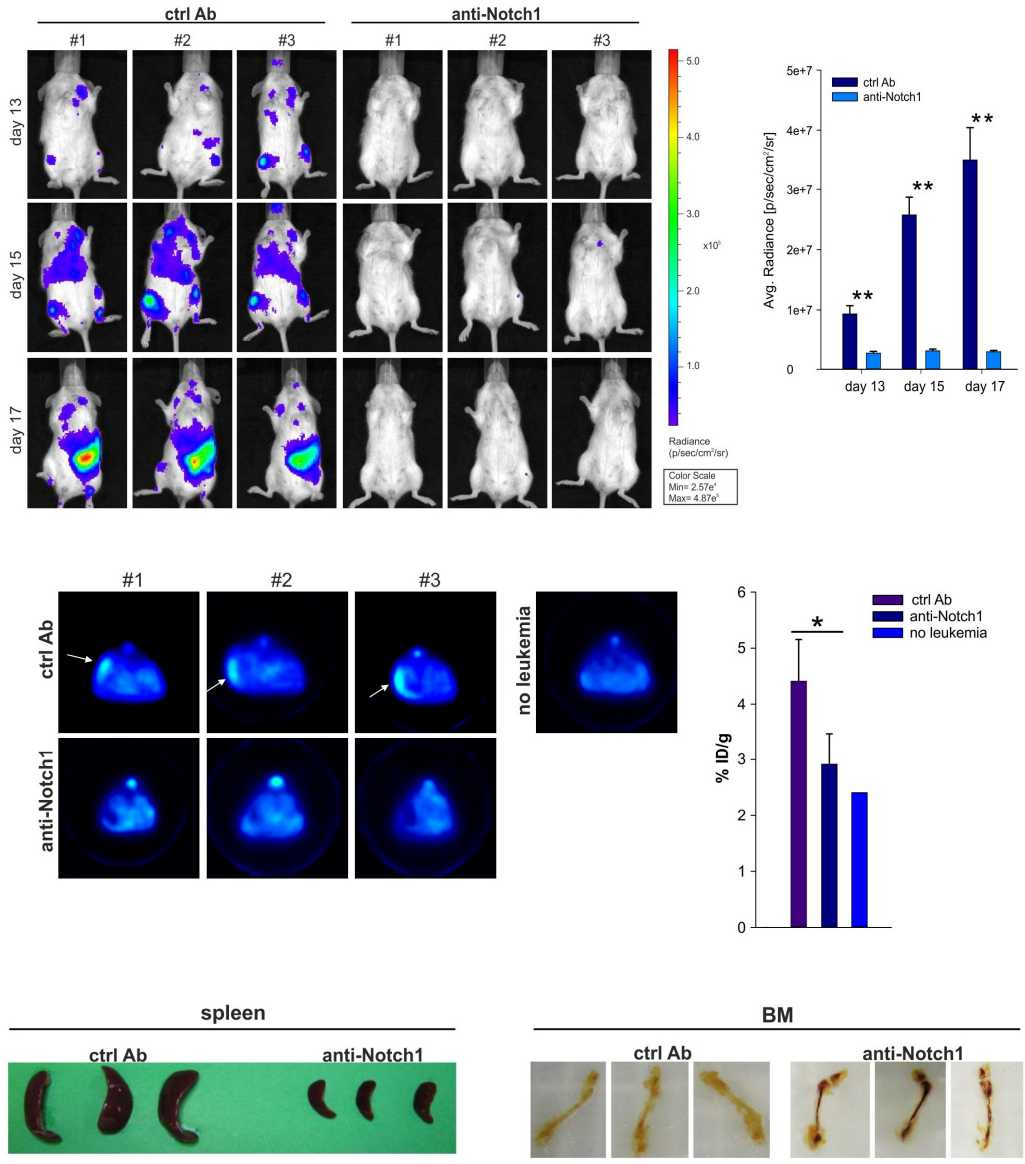

Figure 11: Anti-Notch1 reduces tumor burden in mice bearing human T-ALL cells. **Top:** Optical imaging in PDTALL19 xenografts treated with control Ab or anti-Notch1. PDTALL19 cells were labeled with the luciferase gene and injected i.v. into NOD/SCID mice (5×10^6 cells/mouse; n=5 mice/group). Images acquired at day 13, 15, 17 after cells injection of three representative ctrl Ab- or anti-Notch1 treated mice are reported. On the right, quantitative analysis of luciferase activity *in vivo* at the same time points of measurement (n=5 mice/group). Statistically significant differences in average radiance in the two groups of samples are indicated (**P<0.001).**Middle:** Representative images of [^{18}F]FDG-PET analysis of control antibody- and anti-Notch1-treated PDTALL19 xenografts (n=5 mice/group). NOD/SCID mice without leukemia were used as control (n=3). Measurements of [^{18}F]FDG uptake in the analyzed mice are reported in the graph, expressed as percentage of injected dose per gram of tissue (%ID/g). and statistically significant differences in the two groups of samples are indicated (*P<0.05). White arrows indicate highly glycolytic spleens. **Bottom:** Macroscopic features of spleen and femurs from ctrl Ab- or anti-Notch1 treated mice. Leukemia outgrowth is accompanied by splenomegaly and pale appearance of BM, two pathologic features which are lacking in anti-Notch1 treated mice.

Given such promising results, we investigated whether anti-Notch1 therapy was effective also in mice with advanced disease. In this setting, mice bearing about 5% leukemia cells in the spleen and nearly 25% in the BM received 2 i.p. injections of anti-Notch1 mAb on day 11 and day 17 after cells injection (Fig. 12, top panel). Blood drawings showed that levels of circulating blasts increased in control mice whereas they remained stable in anti-Notch1-treated animals. At sacrifice, anti-Notch1-treated mice had significantly lower levels of leukemic cells in the spleen and BM (Fig. 12, bottom panel).

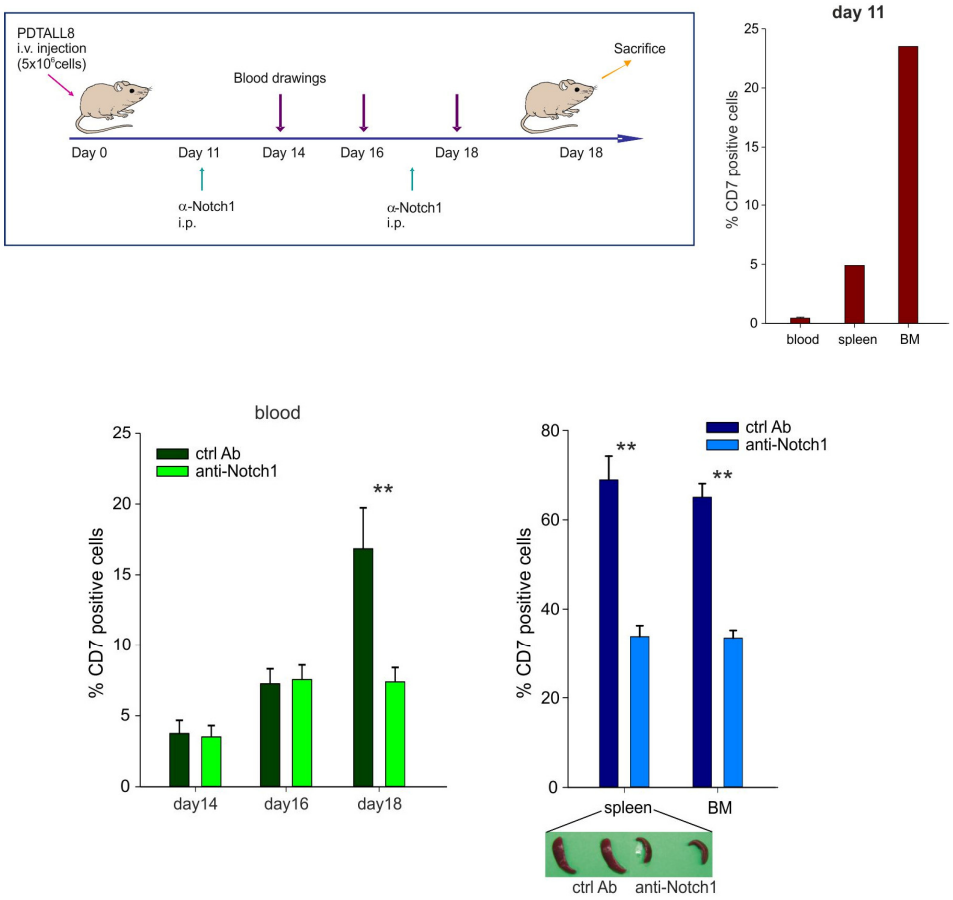

Figure 12: Therapeutic effects of anti-Notch1 therapy in the advanced disease setting. **Top:** Outline of late intervention treatment with anti-Notch1 or control antibody (ctrl Ab) in PDTALL8 xenografts (n=6 mice/group) (left panel). Treatment was started 11 days after i.v. injection of T-ALL cells, when various levels of leukemia cells were detected in the blood, spleen and BM of the mice (right panel, n=3 mice). **Bottom:** Measurement of leukemia cells in the blood at different time points (left). Levels of T-ALL cells recovered in the spleen and BM at sacrifice and picture of the spleen in control and anti-Notch1-treated mice (right). Statistically significant differences in the two groups of samples are indicated (** P<0.001).

4.4 Analysis of the effects of anti-Notch1 mAb on gene expression

To assess whether anti-leukemia effects were in fact due to blockade of Notch signaling, we measured levels of a set of Notch-target transcripts by TaqMan®Arrays. To this end, we sorted leukemic $CD5^+$ cells from either spleen or BM of anti-Notch1-treated or control mice and extracted RNA from these pooled samples. Results showed that the therapeutic response was associated with a strong inhibition of Notch signaling, as depicted in figure 13. In particular four genes (*CR2*, *DTX1*, *HES1* and *HES4*) emerged as markedly attenuated following treatment, suggesting them as sentinel genes of the therapeutic response. Interesting, similar results in terms of gene expression were obtained in mice receiving anti-Notch1 therapy as an early or a late therapeutic protocol.

On the contrary, in poor responders several Notch-related transcripts were poorly expressed and their expression levels were minimally perturbed by anti-Notch1 therapy. Among these genes, *DTX1*, *HES4* and *NOTCH3* were undetectable as opposed to high expression in good responders, fitting with their features of sentinel genes. The transcriptional profile of PDTALL13 following anti-Notch1 therapy is reported in figure 13 and very similar results were obtained with PDTALL16, another poor-responder (data not shown).

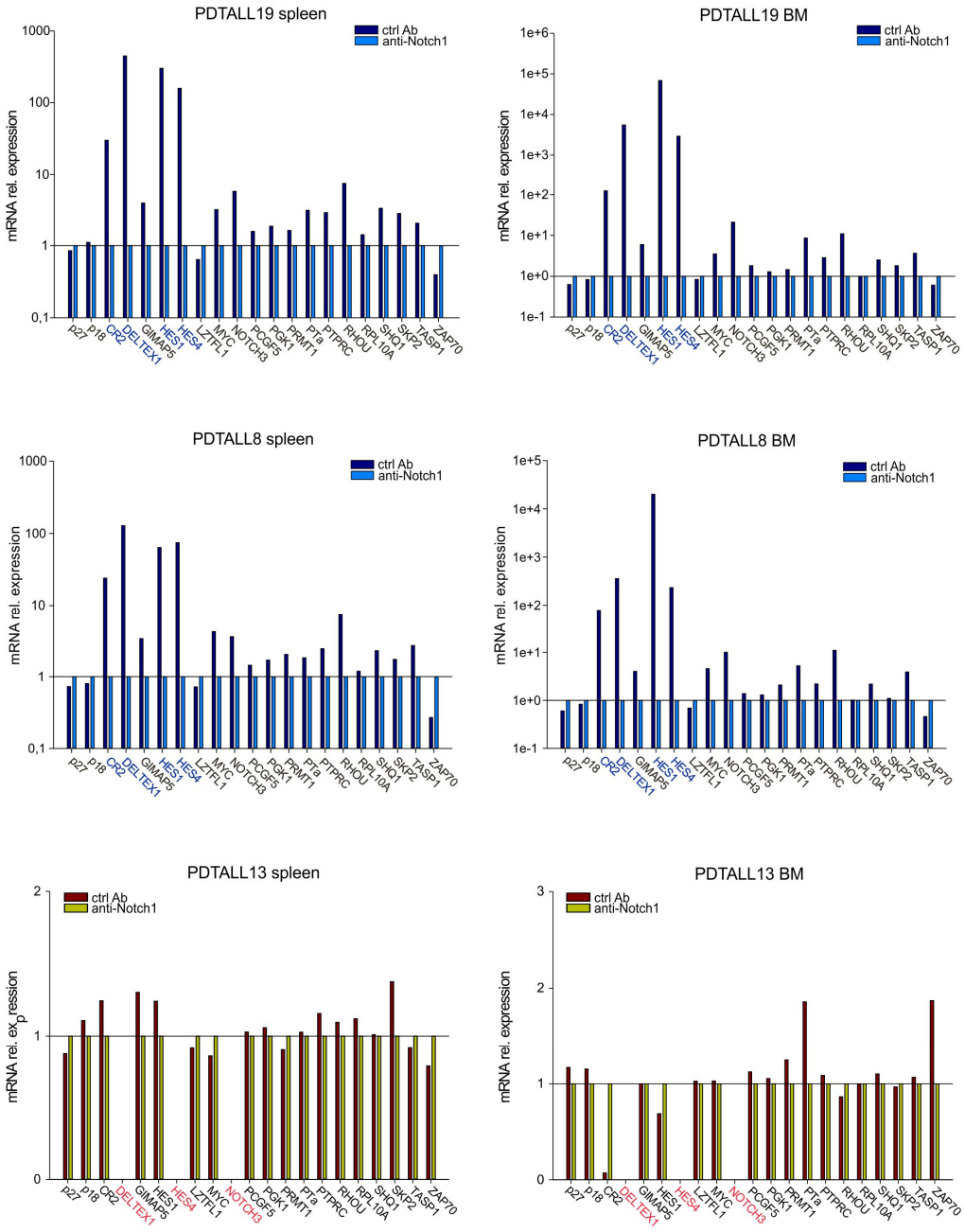

Figure 13: Anti-Notch1 therapy inhibits Notch signaling in T-ALL xenografts. Human CD5^{+} cells were sorted from spleen and BM of anti-Notch1 treated or control mice, pooled (n=3-6 samples per pool) and utilized to investigate effects on Notch signaling. Expression levels of 21 Notch-target genes were measured using Low Density qRT-PCR Arrays. **Top:** Gene expression profile in PDTALL19 xenograft, a representative example of an anti-Notch1 good responder. Treatment - initiated at day 2 - was highly effective in inhibiting expression of Notch target genes both in spleen and in BM. **Middle:** Gene expression profile in PDTALL8 xenograft in the late intervention trial, in which therapy was started at day 11 **Bottom:**. Gene expression profile in PDTALL13, a xenograft which does not respond to anti-Notch1 therapy.

Since we observed such a clear distinction between the transcriptional profile of anti-Notch1 good and poor responders, we wondered if anti-Notch1 therapy could affected other cellular pathways and genes. With this concept in mind, we performed Affymetrix gene expression analysis from pools of PDTALL19 cells purified from the BM of mice treated with anti-Notch1 or control mAbs (3 replicates). The global overview of the highly significantly modulated transcripts confirmed results obtained with TaqMan®Arrays, indicating a marked reduction in expression levels of several canonical Notch target genes such as *CR2*, *DTX1*, *HES1* and *NOTCH3* (Fig. 14).

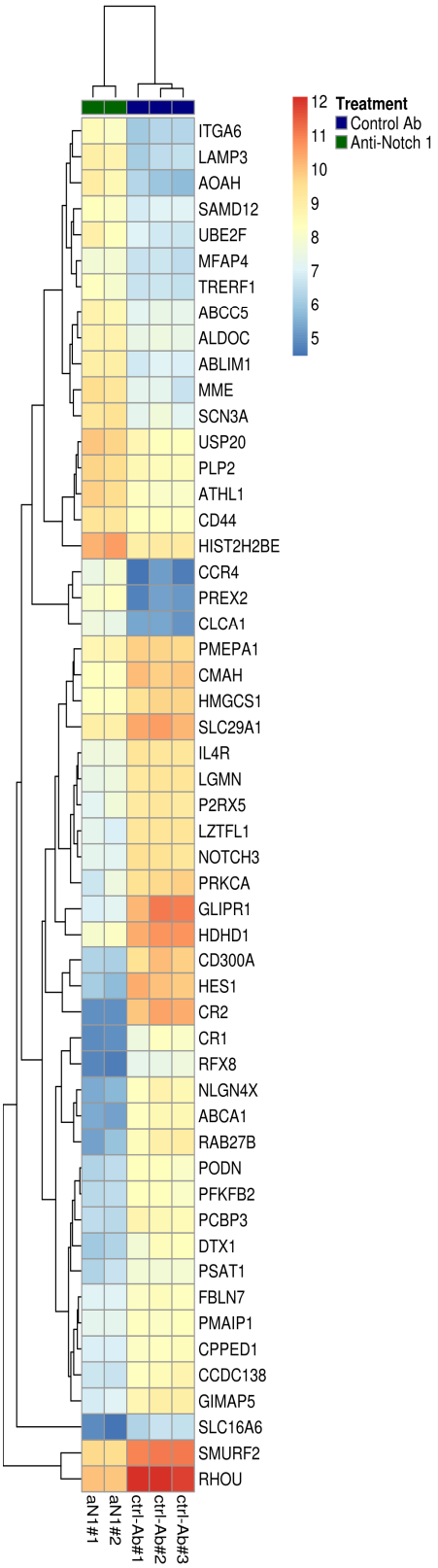

Figure 14: Global changes in gene expression profile following anti-Notch1 therapy in leukemia-bearing mice. Here is reported the heat map of top 53 significant genes that turn out to be up- or down-regulated with BH adjusted p-value< 0.002. Hierarchical clustering of genes (rows) and samples (columns) is based on Euclidean distance metric and complete linkage method while color coding is used to represent absolute gene expression levels, the largest expression values are displayed in red (hot), the smallest values in blue (cool). Clustering on samples was also used as a preliminary quality control. Genes are grouped in two main clusters representing up- and down-regulated genes in antiNotch1 (aN1) vs. control antibody (ctrl Ab); two up-regulated genes (*SMURF2* and *RHOU*) are clustering separately due to gene expression levels very different from the corresponding groups.

Moreover, Affymetrix arrays disclosed that Notch1 blockade modulates expression of several transcripts involved in metabolic functions, such as glycolysis-associated genes (*PFKFB2*, *ALDOC*), membrane carriers (*SLC29A1*, *SLC16A6*), and channels (*CLCA1*, *SCN3A*) (Fig. 14). Intrigued by these data, we performed a preliminary experiment in which we detected the uptake of a fluorescent glucose analog (2-NBDG) in PDTALL8-bearing mice treated with control Ab or anti-Notch1. As shown in figure 15, T-ALL cells recovered from anti-Notch1-treated mice captured less 2-NBDG compared to control Ab-treated mice both in spleen and BM. These preliminary findings fit with the well-established activity of Notch signaling on cellular metabolism (Palomero et al., 2006).

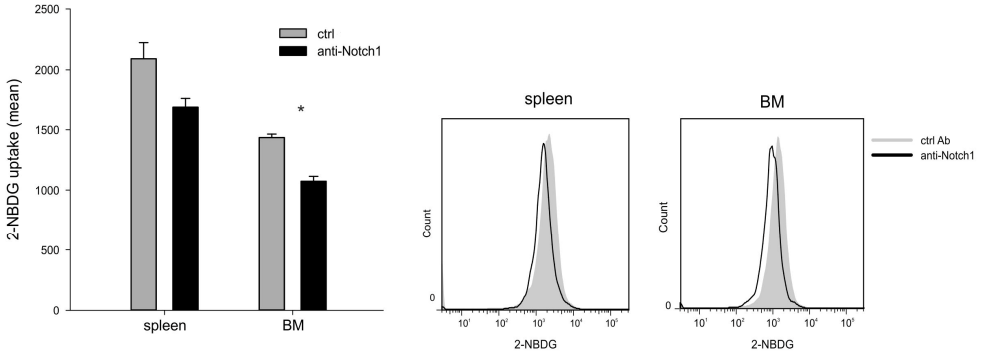

Figure 15: Anti-Notch1 therapy decreases glucose uptake. **Left:** Measurements of 2-NBDG uptake by T-ALL cells in spleen and BM of mice treated with control or anti-Notch1 Abs. (*: p=0.002). **Right:** One representative example of flow cytometric analysis of glucose uptake in spleen and BM. [2-NBDG = 2-N-[(7-nitrobenz-2-oxa-1,3-diazol-4-yl)amino]-2-deoxy-D-glucose]

Gene set enrichment analysis (GSEA) highlighted that the most relevant effects of anti-Notch1 on coordinated groups of genes were mainly in the sense of down-regulation, specifically 36 up- and 374 down-regulated gene sets were identified (false discovery rate FDR q-value < 0.05). Interestingly, among the top list of down-regulated gene sets we noticed several gene sets representing MYC targets, confirming the role of MYC as important mediator of Notch1 activity (Palomero et al., 2006; Sharma et al., 2006; Weng et al., 2006). Restricting our attention to KEGG pathways, we identified 22 significantly down-regulated pathways (Table III) and no significant up-regulated pathways with FDR q-value < 0.05. Moreover,

GSEA was used to evaluate the significance of sets of genes, grouped together by biological process as defined in the Gene Ontology. The analysis disclosed 12 biological process significantly down-regulated, reported in Table III.

#	Name of KEGG pathway significantly down-regulated	SIZE	NES	FDR q-val
1	DNA_REPLICATION	32	-2,29	0,0011
2	PROTEASOME	36	-2,27	0,0006
3	PURINE_METABOLISM	102	-2,19	0,0004
4	PYRIMIDINE_METABOLISM	73	-2,09	0,0021
5	NOTCH_SIGNALING_PATHWAY	36	-2,07	0,0031
6	COMPLEMENT_AND_COAGULATION_CASCADES	19	-2,01	0,0060
7	GLUTATHIONE_METABOLISM	31	-1,99	0,0055
8	CELL_CYCLE	98	-1,93	0,0081
9	AMINOACYL_TRNA_BIOSYNTHESIS	38	-1,88	0,0124
10	HOMOLOGOUS_RECOMBINATION	21	-1,84	0,0169
11	BASE_EXCISION_REPAIR	27	-1,81	0,0194
12	PYRUVATE_METABOLISM	30	-1,80	0,0205
13	CYSTEINE_AND_METHIONINE_METABOLISM	23	-1,80	0,0201
14	RIBOSOME	49	-1,77	0,0234
15	RNA_POLYMERASE	24	-1,77	0,0220
16	ARGININE_AND_PROLINE_METABOLISM	24	-1,75	0,0266
17	NUCLEOTIDE_EXCISION_REPAIR	37	-1,73	0,0293
18	MISMATCH_REPAIR	21	-1,73	0,0281
19	DRUG_METABOLISM_OTHER_ENZYMES	15	-1,72	0,0295
20	AMINO_SUGAR_AND_NUCLEOTIDE_SUGAR_METABOLISM	30	-1,70	0,0341
21	GLYCINE_SERINE_AND_THREONINE_METABOLISM	21	-1,66	0,0469
22	HEMATOPOIETIC_CELL_LINEAGE	45	-1,64	0,0496

#	GO biological process significantly down-regulated	SIZE	NES	FDR q-val
1	DNA_DEPENDENT_DNA_REPLICATION	42	-2,09	0,0095
2	PROTEIN_FOLDING	46	-2,11	0,0124
3	DNA_REPLICATION	77	-2,04	0,0138
4	DNA_DAMAGE_RESPONSE SIGNAL_TRANSDUCTION	21	-1,95	0,0223
5	TRNA_METABOLIC_PROCESS	16	-1,98	0,0231
6	NUCLEO BASE NUCLEOSIDE_AND_NUCLEOTIDE_METABOLIC_PROCESS	37	-1,95	0,0252
7	M_PHASE	80	-1,89	0,0253
8	CELLULAR_BIOSYNTHETIC_PROCESS	202	-1,89	0,0256
9	CELL_CYCLE_PROCESS	135	-1,89	0,0270
10	CELL_CYCLE_PHASE	120	-1,90	0,0277
11	DNA_METABOLIC_PROCESS	192	-1,91	0,0295
12	NUCLEOTIDE_METABOLIC_PROCESS	28	-1,91	0,0322

Table III: GSEA results applied to KEGG pathways and to GO biological process gene sets

4.5 Analysis of the effects of anti-Notch1 mAb on leukemia-initiating cells

In the last years, different groups have studied various subsets of leukemic cells in order to identify leukemia initiating cells (L-IC) that may account for disease progression. Regarding T-ALL, previous studies disclosed that $CD34^+CD4^-CD7^-$ cells might be enriched in L-IC (Cox et al., 2007). However, other groups reported that the $CD34^+CD7^+$ (Gerby et al., 2011) or the $CD7^+CD1a^-$ (Chiu et al., 2010) subsets might contain L-IC. We analyzed expression of these markers by flow cytometry but $CD34^+CD4^-CD7^-$ and $CD34^+CD7^+$ were almost undetectable (<0.1%) in PDTALL8 and PDTALL19 xenografts and their number did not change following treatment. Since these analysis were low informative, we investigated whether efficacy of anti-Notch1 therapy was associated with reduction of tumorigenic potential by serial transplantation experiments. PDTALL19-bearing mice were treated according to standard early treatment outline. At sacrifice, viable T-ALL cells were FACS sorted from spleen of control Ab- or anti-Notch1-treated mice and injected at 3 different doses ($1x10^5$, $2.5x10^4$, $6.25x10^3$ cells) into naïve NOD/SCID mice (4 mice per group). Recipient mice were not treated and leukemia engraftment was periodically monitored by blood drawings. Mice injected with T-ALL cells from control Ab-treated mice developed full blown leukemia in 27-34 days, depending on the cell dose received. In contrast, in all mice injected with cells obtained from anti-Notch1-treated animals very low percentages of leukemic cells were recovered in the blood and mice seemed healthy. These mice eventually developed leukemia, 10-12 days after the sacrifice of control mice (Fig. 16, top panel). These results suggest that anti-Notch1 therapy reduces leukemia engraftment during the treatment and furthermore impairs the ability of T-ALL cells to re-grow after serial transplantation.

Finally we investigated whether leukemia arising in mice injected with cells from anti-Notch1 treated mice were still responder to anti-Notch1 therapy. These cells were hence injected in naïve mice and were treated with anti-Notch1 or control Ab according to standard protocol. Therapeutic response was comparable to those

measured in previous experiments, suggesting that these cells were still sensitive to anti-Notch1 therapy (Fig 16, bottom panel).

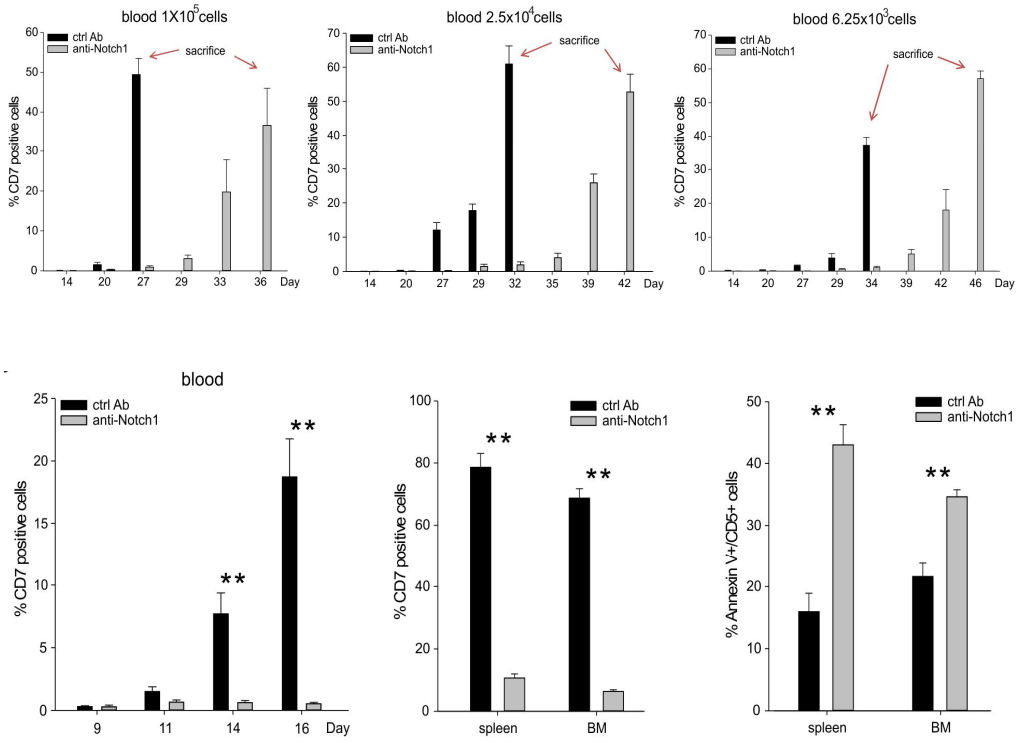

Figure 16: Anti-Notch1 therapy delays T-ALL engraftment. **Top:** Percentages of circulating blasts at different time points in mice injected with serial (1:4) dilutions of human CD5+ cells ($1x10^5$, $2.5x10^4$, $6.25x10^3$ cells/mouse) sorted from the spleen of ctrl Ab and anti-Notch1 treated mice (n=4 mice/group). **Bottom:** Leukemia cells obtained at sacrifice (day 46) from the spleen of mice injected with T-ALL cells from anti-Notch1-treated mice were injected in naive NOD/SCID mice (n=5 mice/group), and two days later these mice were treated with weekly injections of ctrl Ab or anti-Notch1 antibodies. Measurements of circulating blasts are reported in the left panel while percentages of blasts and apoptotic cells at sacrifice are represented in middle and right panel respectively. Statistically significant differences are indicated (** P<0.001).

4.6 Resistance to Notch1-targeted therapy: preliminary data

Xenografts with *NOTCH1* mutations respond well to anti-Notch1 therapy, but are these responses sustained? Do T-ALL cells become resistant to anti-Notch1 therapy? Intrigued by this question, we treated PDTALL19-bearing mice with anti-Notch1 antibody until progression. T-ALL cells engraftment in mice were monitored both by flow cytometric analysis of blood drawings and bioluminescence imaging. 17 days after cells injection, control Ab-treated mice were sacrificed because of widespread leukemia and signs of illness whereas anti-Notch1-treated mice had very low levels of circulating blasts (Fig. 17). However, blood drawings carried out at subsequent time points disclosed growing levels of leukemic cells. Interestingly, even though the percentages of leukemic cells gradually increased, the reduction in the surface CD7 expression was maintained for the entire experiment. Anti-Notch1-treated mice were sacrificed after 6 injections of anti-Notch1 antibody at day 44, that is an increase in the overall survival of 27 days compared to control Ab-treated mice. According to our experience PDTALL19 are very aggressive xenografts, causing leukemia within 14-17 days if injected at ordinary dose ($5x10^6$ cells in experiments). Considering this aspect, an increase in the overall survival of nearly one month can be interpreted as a rather good outcome. We will further investigate the mechanism(s) at the base of resistance, in order to discern whether resistance to Notch1 neutralization could be due to escape mechanisms involving the target (i.e. mutations in the epitope bound by the therapeutic antibody) or selection of T-ALL clones driven by other Notch-unrelated pathways and finally clarify if resistance to anti-Notch1 therapy is a stable trait.

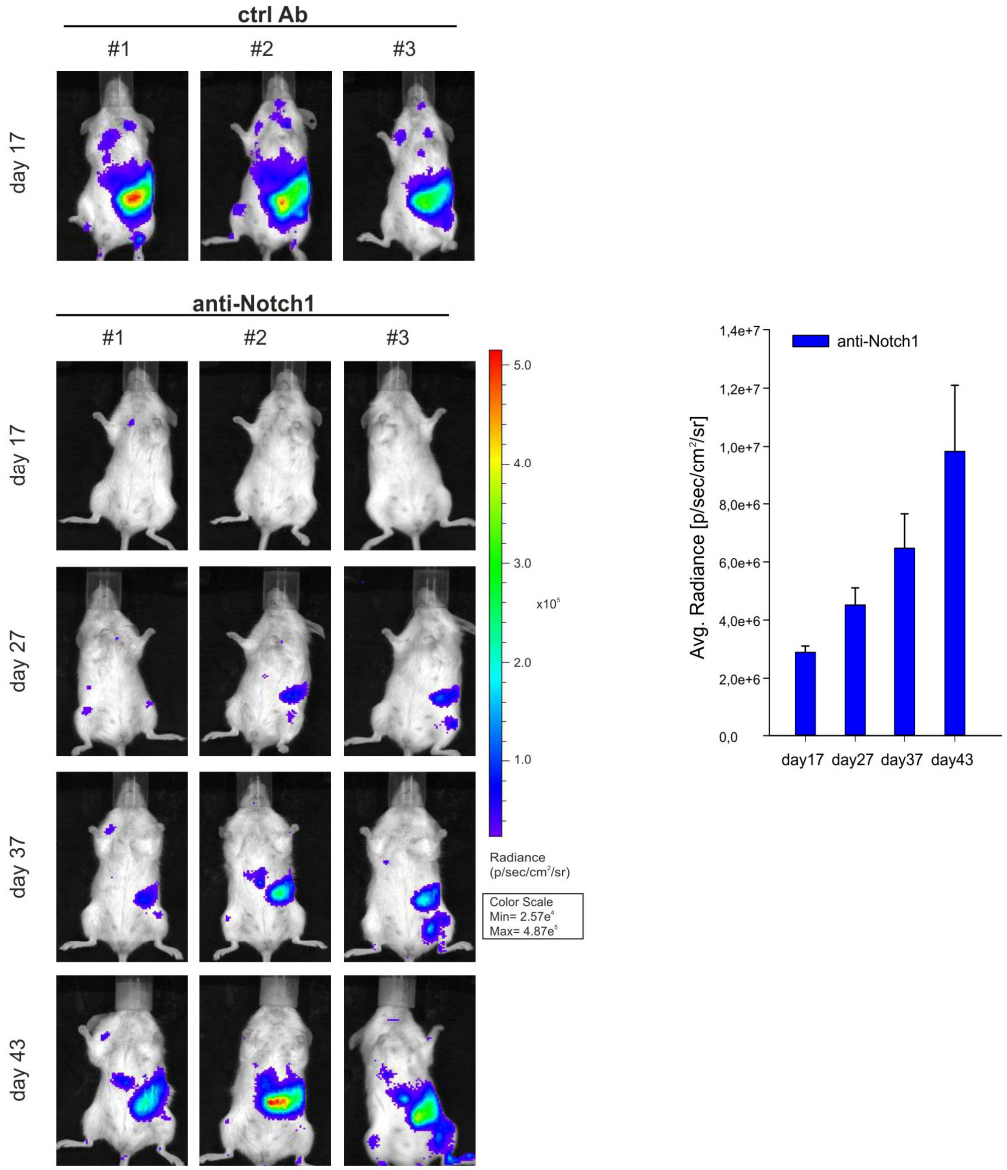

Figure 17: Optical imaging in PDTALL19 xenograft disclosed onset of resistance to Notch1-targeted therapy. PDTALL19 cells were labeled with the luciferase gene and injected i.v. into NOD/SCID mice (5×10^6 cells/mouse; n=5 mice/group). **Top:** The last imaging performed in ctrl Ab-treated mice on day 17, immediately before sacrifice (three representative mice). **Bottom:** Images of three representative anti-Notch1 treated mice captured at different time points (day 17, 27, 37 and 43 after cells injection). On the right, quantitative analysis of luciferase activity in vivo at the same time points of measurement in anti-Notch1-treated mice (n=5 mice).

During preparation of this thesis, the same experiment was repeated with PDTALL12 cells, which were even better responder to anti-Notch1 therapy compared to PDTALL19 cells. Control Ab-treated mice were sacrificed 16 days after cells injection, whereas anti-Notch1-treated mice did not present signs of leukemia up to >75 days later.

4.7 Preliminary experiments about combination of anti-Notch1 mAb and dexamethasone

Our previous results indicate that anti-Notch1 therapy reduces but does not completely block leukemia engraftment or L-IC function, furthermore resistance may arise in a regimen of continuous administration of anti-Notch1 mAb. Combination of drugs might putatively improve therapeutic efficacy, by further reducing leukemia cell burden. In a preliminary experiment, we treated PDTALL8 xenografts either with dexamethasone -a drug commonly used for T-ALL treatment- combined or not with anti-Notch1 (5 mice/group). Anti-Notch1 was administered 11 days after cells injection, as in the late intervention trial, in order to decrease but not totally eliminate leukemia cell engraftment. This residual disease could be further reduced by administration of dexamethasone. Leukemia engraftment was monitored by blood drawings and percentages of blasts and apoptotic cells in spleen and BM were measured at sacrifice. As represented in figure 18, levels of leukemic cells in mice treated with the combination of both drugs were extremely low. Moreover, apoptosis of T-ALL cells was significantly higher in the group receiving the combination of anti-Notch1 and dexamethasone in respect to groups treated with single therapies both in the spleen and in the BM. These findings were further confirmed by comparing weight of the spleen from the various animals (data not shown). This preliminary experiment suggests a potential synergistic effect of anti-Notch1 and dexamethasone treatments, a promising result for future therapeutic applications of anti-Notch1 therapy for T-ALL.

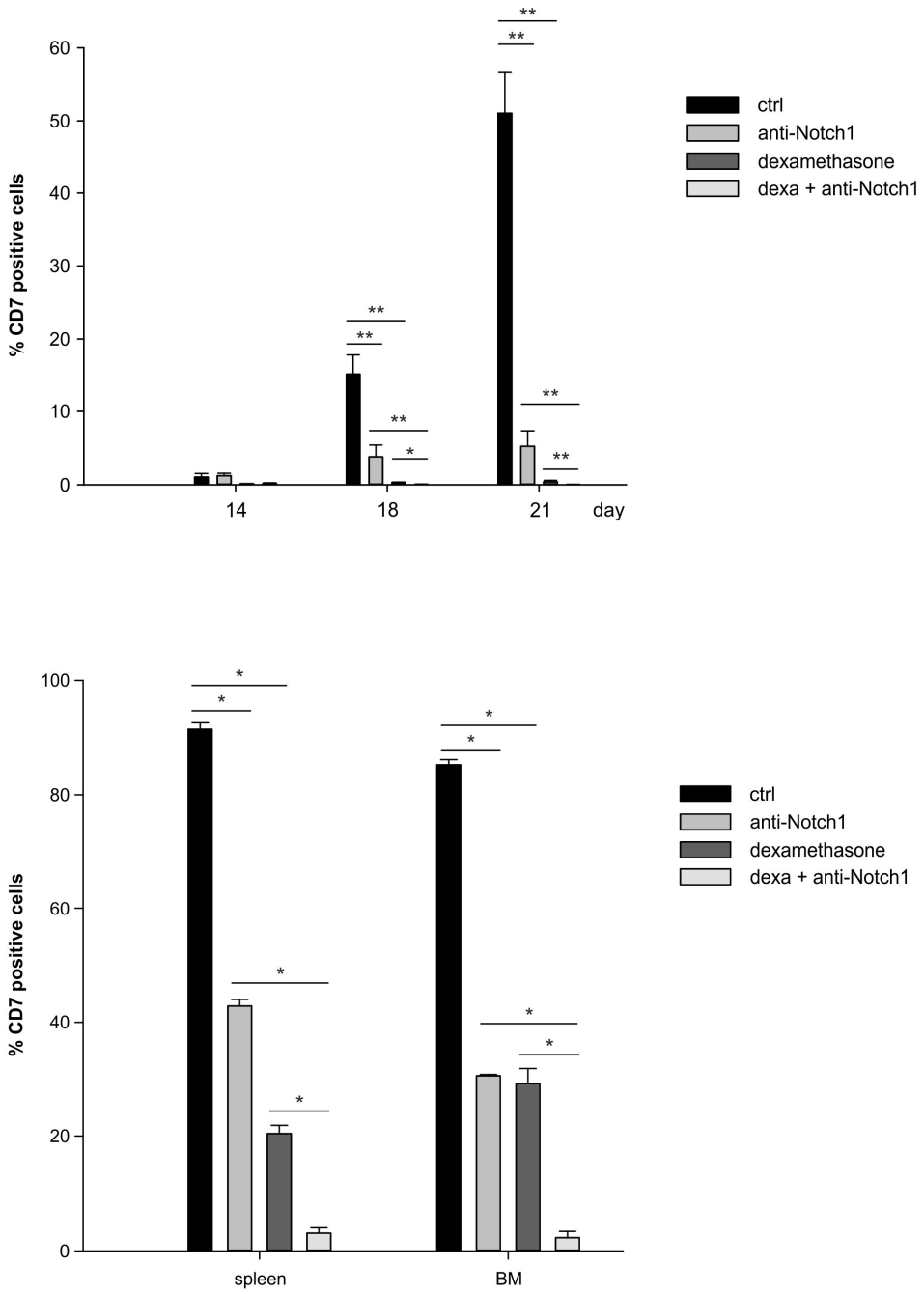

Fig. 18: Combination of dexamethasone and anti-Notch1 mAb impairs leukemia cell engraftment. **Top:** measurements of circulating blasts in mice treated with either control Ab, anti-Notch1, dexamethasone or a combination of both reagents. **Bottom:** Evaluation of leukemic cells in spleen and BM in mice that received one of the treatment reported in the legend. The combination of dexamethasone and anti-Notch1 has stronger therapeutic effect compared to monotherapy.

5. DISCUSSION

Although we are aware of intrinsic limitations of xenografts, the systemic T-ALL model generated in our lab was very useful to investigate the therapeutic activity of a novel neutralizing antibody against Notch1. Earlier studies about Notch-targeted therapies were limited to T-ALL cell lines *in vitro* (Aste-Amezaga et al., 2010) or grown *in vivo* as s.c. tumor xenografts (Wu et al., 2010), a model barely suitable for an hematological disease such as T-ALL. Only a very recent study (Ma et al., 2012) analyzed the effects of another Notch1-specific antibody in a systemic xenograft model of T-ALL. However, this group mainly focused L-IC subpopulations, demonstrating that Notch1-targeted therapy resulted in substantial depletion of $CD34^+CD2^+CD7^+$ cells, and did not investigate mechanisms behind the therapeutic effects and possible predictive biomarkers. On the other hand, xenografts that responded to anti-Notch1 therapy in our study had negligible levels of $CD34^+$ cells, therefore it was not possible to validate the findings of Ma and colleagues in our model.

Our clinically relevant T-ALL model permitted us to study the therapeutic effects of Notch1 blockade in xenografts derived from difficult-to-treat patients, as PDTALL19, which was derived from a relapse, or poor responders to prednisone (PDTALL8, PDTALL11, PDTALL16, PDTALL18, PDTALL19). Anti-Notch1 therapy was effective in several of these xenografts, an encouraging result considering the lack of efficacy of established therapies for poor prognosis T-ALL patients (Coustan-Smith et al., 2009; Zhang et al., 2012). Our results demonstrated that *NOTCH1/FBW7* mutated samples are suitable candidates for Notch1-targeted therapy, since all mutation-bearing xenografts analyzed presented a significant reduction in leukemia engraftment, increased apoptosis levels and a decrease in cell proliferation compared to control mice. Therapeutic efficacy was detected even in the late intervention trial, notwithstanding an involvement of near 25% of BM by leukemia cells at time of drug administration. Differences in apoptosis and proliferation following Notch1 blockade are in line with literature findings with

GSI (Lewis et al., 2007; Weng et al., 2004). Efficacy of anti-Notch1 therapy seemed to be rather independent from the specific mutation, considering that we tested mutations in HD domain (PDTALL11), in PEST (PDTALL12), in HD/PEST (PDTALL8) and HD/TAD plus mutation in FBW7 (PDTALL19) and all were good responders according to results explained above. On the contrary, xenografts with wild-type *NOTCH1* and *FBW7* sequences did not respond to anti-Notch1 treatment. Altogether, our findings clearly demonstrate that *NOTCH1/FBW7* mutations identify responders in xenografts. In future studies, genetic screening could be helpful to stratify patients and identify predictive biomarkers of response to this targeted therapy.

A very interesting result that emerges from our findings is the correlation between the mutational status, the response to anti-Notch1 therapy and the expression of some Notch target genes such as *DTX1*, *HES4* and *NOTCH3*. These genes were absent or undetectable in wt/poor responder xenografts whereas they were highly expressed, and modulated following therapy, in mutated/good responder xenografts, suggesting them as sentinel genes for the therapeutic response. Moreover the efficacy of anti-Notch1 therapy correlated also with surface expression of CD7, since its down-modulation was a stable trait in all responder samples and was confirmed also at transcriptional level by GEP analysis. These data highlight the potential of measurements of Notch target genes and/or CD7 expression as candidate predictive markers of response to anti-Notch1 therapy. CD7 is one of the galectin-1 receptors and is directly regulated by NFκB upon T-cell activation (Koh et al., 2008). It is known that NFκB activation is sustained by Notch pathway and in particular by *HES1* (Espinosa et al., 2010), one of the most important Notch target genes. One hypothesis about down-modulation of CD7 could be the decrease in CD7 expression due to reduced NFκB activity caused in turn by Notch1 blockade. Another possible explanation is that anti-Notch1 treatment could impair growth of $CD7^+$ cells, although cytofluorimetric data do not suggest the existence of distinct CD7 bright and dim cell populations in the samples.

Since Notch1 is expressed by leukemia cells, we planned to investigate the *in vitro* effects of anti-Notch1 antibody in order to further clarify the mechanism of the therapeutic effect. Unfortunately, the primary T-ALL cells derived from xenografts stop growing and tend to die quite rapidly *in vitro*, thus preventing the possibility of performing these experiments.

The experiment with PDTALL19 xenograft disclosed that resistance may arise following prolonged anti-Notch1 therapy. Our systemic T-ALL model can also be utilized to investigate mechanisms of acquired resistance to Notch1-targeted therapy. We are indeed interested in understanding whether there is selection of a Notch-independent population sustained by other signaling pathways or if the escape mechanism involves the target (i.e. mutations in the epitope bound by the therapeutic antibody). Moreover, it will be important to investigate whether resistance is a stable trait or if T-ALL cells can still respond to anti-Notch1 therapy upon serial transplantation in naive mice. Based on literature studies, some mutations, such as *FBW7* or *PTEN* loss of function, correlate with resistance to GSI treatment in vitro (O'Neil et al., 2007; Palomero et al., 2007), so it will be important to check this possibility in our xenografts. Probably the finding of mutated *FBW7* in PDTALL19 cells -which developed resistance to Notch inhibition- and wild-type *FBW7* in PDTALL12 cells –which are still sensitive to Notch inhibition- is not a coincidence.

Besides possible therapeutic implications, our study might be useful to improve knowledge about Notch signaling and its downstream pathways and genes.

Results obtained by transcriptome analysis following Notch1 blockade disclosed the involvement of different genes of metabolic functions. It is known from the literature that Notch1 directly regulates *c-MYC* through a feed-forward-loop (Palomero et al., 2006) so it was not surprising to observed a modulation of the expression of c-MYC transcripts following anti-Notch1 therapy in our experiments. Moreover, a preliminary experiment suggested that anti-Notch1 therapy compromised glucose uptake by leukemic cells, laying the foundations for future developments about anti-Notch1-mediated effect on cellular metabolism in

our model. Even PET analysis displayed a reduction in the [^{18}F]FDG uptake in anti-Notch1-treated animals compare to control mice, but this result could be also explained by lower numbers of T-ALL cells infiltrating mouse organs, as shown by other techniques.

Anti-Notch1 therapy reduced but did not completely block leukemia engraftment or L-IC function and residual cells maintained the potential to generate leukemia following serial transplantation (Fig. 16). Furthermore, resistance may arise in a regimen of continuous administration, as disclosed by the experiment with PDTALL19 cells. Therefore anti-Notch1 therapy alone may be not sufficient to achieve leukemia regression and therapeutic efficacy could be further improved by combination with steroids and other conventional drugs. In a preliminary experiment we combined the administration of anti-Notch1 with dexamethasone and the results were very encouraging, suggesting a cooperation between the novel antibody and the drug commonly administrated to T-ALL patients (Fig. 18). Findings are in line with recent evidences that Notch inhibition by GSI increased sensitivity to dexamethasone in T-ALL cells (Real et al., 2009). It should be noted that our antibody is specific only for Notch1 receptor, so its therapeutic application should overcome the severe toxicity associated with GSI administration, due to simultaneous blockade of all Notch receptors (Riccio et al., 2008). In future we will implement our studies on combination of anti-Notch1 and other drugs by extending analysis to other xenografts. If the synergistic effect of anti-Notch1 and dexamethasone therapies will be confirmed, results will implement design of future clinical trials.

Finally anti-Notch1 therapy could be extended also to other pathologic conditions where inhibition of Notch signaling is required, such as chronic lymphocytic leukemia (Fabbri et al., 2011) and mantle cell lymphoma (Kridel et al., 2012), hematological diseases in which activating mutations in *NOTCH1* are frequent and are associated with poor clinical prognosis.

6. REFERENCES

Aifantis, I., Raetz, E., and Buonamici, S. (2008). Molecular pathogenesis of T-cell leukaemia and lymphoma. Nat Rev Immunol *8*, 380-390.

Aste-Amezaga, M., Zhang, N., Lineberger, J. E., Arnold, B. A., Toner, T. J., Gu, M., Huang, L., Vitelli, S., Vo, K. T., Haytko, P.*, et al.* (2010). Characterization of Notch1 antibodies that inhibit signaling of both normal and mutated Notch1 receptors. PLoS One *5*, e9094.

Aster, J. C., and Blacklow, S. C. (2012). Targeting the Notch pathway: twists and turns on the road to rational therapeutics. J Clin Oncol *30*, 2418-2420.

Aster, J. C., Pear, W. S., and Blacklow, S. C. (2008). Notch signaling in leukemia. Annu Rev Pathol *3*, 587-613.

Balint, K., Xiao, M., Pinnix, C. C., Soma, A., Veres, I., Juhasz, I., Brown, E. J., Capobianco, A. J., Herlyn, M., and Liu, Z. J. (2005). Activation of Notch1 signaling is required for beta-catenin-mediated human primary melanoma progression. J Clin Invest *115*, 3166-3176.

Beverly, L. J., and Capobianco, A. J. (2003). Perturbation of Ikaros isoform selection by MLV integration is a cooperative event in Notch(IC)-induced T cell leukemogenesis. Cancer Cell *3*, 551-564.

Bin Hafeez, B., Adhami, V. M., Asim, M., Siddiqui, I. A., Bhat, K. M., Zhong, W., Saleem, M., Din, M., Setaluri, V., and Mukhtar, H. (2009). Targeted knockdown of Notch1 inhibits invasion of human prostate cancer cells concomitant with inhibition of matrix metalloproteinase-9 and urokinase plasminogen activator. Clin Cancer Res *15*, 452-459.

Brepoels, L., Stroobants, S., Vandenberghe, P., Spaepen, K., Dupont, P., Nuyts, J., Bormans, G., Mortelmans, L., Verhoef, G., and De Wolf-Peeters, C. (2007). Effect of corticosteroids on 18F-FDG uptake in tumor lesions after chemotherapy. J Nucl Med *48*, 390-397.

Chan, S. M., Weng, A. P., Tibshirani, R., Aster, J. C., and Utz, P. J. (2007). Notch signals positively regulate activity of the mTOR pathway in T-cell acute lymphoblastic leukemia. Blood *110*, 278-286.

Chiu, P. P., Jiang, H., and Dick, J. E. (2010). Leukemia-initiating cells in human T-lymphoblastic leukemia exhibit glucocorticoid resistance. Blood *116*, 5268-5279.

Coustan-Smith, E., Mullighan, C. G., Onciu, M., Behm, F. G., Raimondi, S. C., Pei, D., Cheng, C., Su, X., Rubnitz, J. E., Basso, G., *et al.* (2009). Early T-cell precursor leukaemia: a subtype of very high-risk acute lymphoblastic leukaemia. Lancet Oncol *10*, 147-156.

Cox, C. V., Martin, H. M., Kearns, P. R., Virgo, P., Evely, R. S., and Blair, A. (2007). Characterization of a progenitor cell population in childhood T-cell acute lymphoblastic leukemia. Blood *109*, 674-682.

Di Ianni, M., Baldoni, S., Rosati, E., Ciurnelli, R., Cavalli, L., Martelli, M. F., Marconi, P., Screpanti, I., and Falzetti, F. (2009). A new genetic lesion in B-CLL: a NOTCH1 PEST domain mutation. Br J Haematol *146*, 689-691.

Dik, W. A., Brahim, W., Braun, C., Asnafi, V., Dastugue, N., Bernard, O. A., van Dongen, J. J., Langerak, A. W., Macintyre, E. A., and Delabesse, E. (2005). CALM-AF10+ T-ALL expression profiles are characterized by overexpression of HOXA and BMI1 oncogenes. Leukemia *19*, 1948-1957.

Dohda, T., Maljukova, A., Liu, L., Heyman, M., Grander, D., Brodin, D., Sangfelt, O., and Lendahl, U. (2007). Notch signaling induces SKP2 expression and promotes reduction of p27Kip1 in T-cell acute lymphoblastic leukemia cell lines. Exp Cell Res *313*, 3141-3152.

Dumortier, A., Jeannet, R., Kirstetter, P., Kleinmann, E., Sellars, M., dos Santos, N. R., Thibault, C., Barths, J., Ghysdael, J., Punt, J. A., *et al.* (2006). Notch activation is an early and critical event during T-Cell leukemogenesis in Ikaros-deficient mice. Mol Cell Biol *26*, 209-220.

Ellisen, L. W., Bird, J., West, D. C., Soreng, A. L., Reynolds, T. C., Smith, S. D., and Sklar, J. (1991). TAN-1, the human homolog of the Drosophila notch gene, is broken by chromosomal translocations in T lymphoblastic neoplasms. Cell *66*, 649-661.

Espinosa, L., Cathelin, S., D'Altri, T., Trimarchi, T., Statnikov, A., Guiu, J., Rodilla, V., Ingles-Esteve, J., Nomdedeu, J., Bellosillo, B., *et al.* (2010). The Notch/Hes1 pathway sustains NF-kappaB activation through CYLD repression in T cell leukemia. Cancer Cell *18*, 268-281.

Fabbri, G., Rasi, S., Rossi, D., Trifonov, V., Khiabanian, H., Ma, J., Grunn, A., Fangazio, M., Capello, D., Monti, S., *et al.* (2011). Analysis of the chronic lymphocytic leukemia coding genome: role of NOTCH1 mutational activation. J Exp Med *208*, 1389-1401.

Ferrando, A. A., Neuberg, D. S., Staunton, J., Loh, M. L., Huard, C., Raimondi, S. C., Behm, F. G., Pui, C. H., Downing, J. R., Gilliland, D. G., *et al.* (2002). Gene expression signatures define novel oncogenic pathways in T cell acute lymphoblastic leukemia. Cancer Cell *1*, 75-87.

Fielding, A. K., Banerjee, L., and Marks, D. I. (2012). Recent developments in the management of T-cell precursor acute lymphoblastic leukemia/lymphoma. Curr Hematol Malig Rep *7*, 160-169.

Gentleman, R. C., Carey, V. J., Bates, D. M., Bolstad, B., Dettling, M., Dudoit, S., Ellis, B., Gautier, L., Ge, Y., Gentry, J.*, et al.* (2004). Bioconductor: open software development for computational biology and bioinformatics. Genome Biol *5*, R80.

Gerby, B., Clappier, E., Armstrong, F., Deswarte, C., Calvo, J., Poglio, S., Soulier, J., Boissel, N., Leblanc, T., Baruchel, A.*, et al.* (2011). Expression of CD34 and CD7 on human T-cell acute lymphoblastic leukemia discriminates functionally heterogeneous cell populations. Leukemia *25*, 1249-1258.

Germano, G., Songia, S., Biondi, A., and Basso, G. (2001). Rapid detection of clonality in patients with acute lymphoblastic leukemia. Haematologica *86*, 382-385.

Ikawa, T., Kawamoto, H., Goldrath, A. W., and Murre, C. (2006). E proteins and Notch signaling cooperate to promote T cell lineage specification and commitment. J Exp Med *203*, 1329-1342.

Inaba, H., and Pui, C. H. (2010). Glucocorticoid use in acute lymphoblastic leukaemia. Lancet Oncol *11*, 1096-1106.

Koh, H. S., Lee, C., Lee, K. S., Ham, C. S., Seong, R. H., Kim, S. S., and Jeon, S. H. (2008). CD7 expression and galectin-1-induced apoptosis of immature thymocytes are directly regulated by NF-kappaB upon T-cell activation. Biochem Biophys Res Commun *370*, 149-153.

Kopan, R., and Ilagan, M. X. (2009). The canonical Notch signaling pathway: unfolding the activation mechanism. Cell *137*, 216-233.

Krak, N. C., Boellaard, R., Hoekstra, O. S., Twisk, J. W., Hoekstra, C. J., and Lammertsma, A. A. (2005). Effects of ROI definition and reconstruction method on quantitative outcome and applicability in a response monitoring trial. Eur J Nucl Med Mol Imaging *32*, 294-301.

Kraszewska, M. D., Dawidowska, M., Larmonie, N. S., Kosmalska, M., Sedek, L., Szczepaniak, M., Grzeszczak, W., Langerak, A. W., Szczepanski, T., and Witt, M. (2012a). DNA methylation pattern is altered in childhood T-cell acute lymphoblastic leukemia patients as compared with normal thymic subsets: insights into CpG island methylator phenotype in T-ALL. Leukemia *26*, 367-371
.

Kraszewska, M. D., Dawidowska, M., Szczepanski, T., and Witt, M. (2012b). T-cell acute lymphoblastic leukaemia: recent molecular biology findings. Br J Haematol *156*, 303-315.
Kridel, R., Meissner, B., Rogic, S., Boyle, M., Telenius, A., Woolcock, B., Gunawardana, J., Jenkins, C., Cochrane, C., Ben-Neriah, S.*, et al.* (2012). Whole transcriptome sequencing reveals recurrent NOTCH1 mutations in mantle cell lymphoma. Blood *119*, 1963-1971.

Lee, S. Y., Kumano, K., Nakazaki, K., Sanada, M., Matsumoto, A., Yamamoto, G., Nannya, Y., Suzuki, R., Ota, S., Ota, Y.*, et al.* (2009). Gain-of-function mutations and copy number increases of Notch2 in diffuse large B-cell lymphoma. Cancer Sci *100*, 920-926.

Lewis, H. D., Leveridge, M., Strack, P. R., Haldon, C. D., O'Neil, J., Kim, H., Madin, A., Hannam, J. C., Look, A. T., Kohl, N.*, et al.* (2007). Apoptosis in T cell acute lymphoblastic leukemia cells after cell cycle arrest induced by pharmacological inhibition of notch signaling. Chem Biol *14*, 209-219.

Lopez-Nieva, P., Santos, J., and Fernandez-Piqueras, J. (2004). Defective expression of Notch1 and Notch2 in connection to alterations of c-Myc and Ikaros in gamma-radiation-induced mouse thymic lymphomas. Carcinogenesis *25*, 1299-1304.

Ma, W., Gutierrez, A., Goff, D. J., Geron, I., Sadarangani, A., Jamieson, C. A., Court, A. C., Shih, A. Y., Jiang, Q., Wu, C. C.*, et al.* (2012). NOTCH1 signaling promotes human T-cell acute lymphoblastic leukemia initiating cell regeneration in supportive niches. PLoS One *7*, e39725.

Mavrakis, K. J., Van Der Meulen, J., Wolfe, A. L., Liu, X., Mets, E., Taghon, T., Khan, A. A., Setty, M., Rondou, P., Vandenberghe, P.*, et al.* (2011). A cooperative microRNA-tumor suppressor gene network in acute T-cell lymphoblastic leukemia (T-ALL). Nat Genet *43*, 673-678.

National Cancer Institute web site:
http://www.cancer.gov/cancertopics/pdq/treatment/childALL/HealthProfessional

O'Neil, J., Grim, J., Strack, P., Rao, S., Tibbitts, D., Winter, C., Hardwick, J., Welcker, M., Meijerink, J. P., Pieters, R.*, et al.* (2007). FBW7 mutations in leukemic cells mediate NOTCH pathway activation and resistance to gamma-secretase inhibitors. J Exp Med *204*, 1813-1824.

Palomero, T., Lim, W. K., Odom, D. T., Sulis, M. L., Real, P. J., Margolin, A., Barnes, K. C., O'Neil, J., Neuberg, D., Weng, A. P.*, et al.* (2006). NOTCH1 directly regulates c-MYC and activates a feed-forward-loop transcriptional network promoting leukemic cell growth. Proc Natl Acad Sci U S A *103*, 18261-18266.

Palomero, T., Sulis, M. L., Cortina, M., Real, P. J., Barnes, K., Ciofani, M., Caparros, E., Buteau, J., Brown, K., Perkins, S. L., *et al.* (2007). Mutational loss of PTEN induces resistance to NOTCH1 inhibition in T-cell leukemia. Nat Med *13*, 1203-1210.

Pirot, N., Deleuze, V., El-Hajj, R., Dohet, C., Sablitzky, F., Couttet, P., Mathieu, D., and Pinet, V. (2010). LYL1 activity is required for the maturation of newly formed blood vessels in adulthood. Blood *115*, 5270-5279.

Puente, X. S., Pinyol, M., Quesada, V., Conde, L., Ordonez, G. R., Villamor, N., Escaramis, G., Jares, P., Bea, S., Gonzalez-Diaz, M., *et al.* (2011). Whole-genome sequencing identifies recurrent mutations in chronic lymphocytic leukaemia. Nature *475*, 101-105.

Pui, C. H., and Evans, W. E. (2006). Treatment of acute lymphoblastic leukemia. N Engl J Med *354*, 166-178.

Pui, C. H., Mullighan, C. G., Evans, W. E., and Relling, M. V. (2012). Pediatric acute lymphoblastic leukemia: where are we going and how do we get there? Blood *120*, 1165-1174.

Radtke, F., Wilson, A., Mancini, S. J., and MacDonald, H. R. (2004). Notch regulation of lymphocyte development and function. Nat Immunol *5*, 247-253.

Real, P. J., Tosello, V., Palomero, T., Castillo, M., Hernando, E., de Stanchina, E., Sulis, M. L., Barnes, K., Sawai, C., Homminga, I., *et al.* (2009). Gamma-secretase inhibitors reverse glucocorticoid resistance in T cell acute lymphoblastic leukemia. Nat Med *15*, 50-58.

Reedijk, M., Odorcic, S., Chang, L., Zhang, H., Miller, N., McCready, D. R., Lockwood, G., and Egan, S. E. (2005). High-level coexpression of JAG1 and NOTCH1 is observed in human breast cancer and is associated with poor overall survival. Cancer Res *65*, 8530-8537.

Riccio, O., van Gijn, M. E., Bezdek, A. C., Pellegrinet, L., van Es, J. H., Zimber-Strobl, U., Strobl, L. J., Honjo, T., Clevers, H., and Radtke, F. (2008). Loss of intestinal crypt progenitor cells owing to inactivation of both Notch1 and Notch2 is accompanied by derepression of CDK inhibitors p27Kip1 and p57Kip2. EMBO Rep *9*, 377-383.

Robinson, D. R., Kalyana-Sundaram, S., Wu, Y. M., Shankar, S., Cao, X., Ateeq, B., Asangani, I. A., Iyer, M., Maher, C. A., Grasso, C. S., *et al.* (2011). Functionally recurrent rearrangements of the MAST kinase and Notch gene families in breast cancer. Nat Med *17*, 1646-1651.

Rodilla, V., Villanueva, A., Obrador-Hevia, A., Robert-Moreno, A., Fernandez-Majada, V., Grilli, A., Lopez-Bigas, N., Bellora, N., Alba, M. M., Torres, F., *et al.*

(2009). Jagged1 is the pathological link between Wnt and Notch pathways in colorectal cancer. Proc Natl Acad Sci U S A *106*, 6315-6320.

Roman-Gomez, J., Jimenez-Velasco, A., Agirre, X., Prosper, F., Heiniger, A., and Torres, A. (2005). Lack of CpG island methylator phenotype defines a clinical subtype of T-cell acute lymphoblastic leukemia associated with good prognosis. J Clin Oncol *23*, 7043-7049.

Sanchez-Irizarry, C., Carpenter, A. C., Weng, A. P., Pear, W. S., Aster, J. C., and Blacklow, S. C. (2004). Notch subunit heterodimerization and prevention of ligand-independent proteolytic activation depend, respectively, on a novel domain and the LNR repeats. Mol Cell Biol *24*, 9265-9273.

Serafin, V., Persano, L., Moserle, L., Esposito, G., Ghisi, M., Curtarello, M., Bonanno, L., Masiero, M., Ribatti, D., Sturzl, M.*, et al.* (2011). Notch3 signalling promotes tumour growth in colorectal cancer. J Pathol *224*, 448-460.

Sharma, V. M., Calvo, J. A., Draheim, K. M., Cunningham, L. A., Hermance, N., Beverly, L., Krishnamoorthy, V., Bhasin, M., Capobianco, A. J., and Kelliher, M. A. (2006). Notch1 contributes to mouse T-cell leukemia by directly inducing the expression of c-myc. Mol Cell Biol *26*, 8022-8031.

Sjolund, J., Johansson, M., Manna, S., Norin, C., Pietras, A., Beckman, S., Nilsson, E., Ljungberg, B., and Axelson, H. (2008). Suppression of renal cell carcinoma growth by inhibition of Notch signaling in vitro and in vivo. J Clin Invest *118*, 217-228.

Smyth, G. K. (2004). Linear models and empirical bayes methods for assessing differential expression in microarray experiments. Stat Appl Genet Mol Biol *3*, Article3.

South, A. P., Cho, R. J., and Aster, J. C. (2012). The double-edged sword of Notch signaling in cancer. Semin Cell Dev Biol *23*, 458-464.

Subramanian, A., Tamayo, P., Mootha, V. K., Mukherjee, S., Ebert, B. L., Gillette, M. A., Paulovich, A., Pomeroy, S. L., Golub, T. R., Lander, E. S., and Mesirov, J. P. (2005). Gene set enrichment analysis: a knowledge-based approach for interpreting genome-wide expression profiles. Proc Natl Acad Sci U S A *102*, 15545-15550.

Sulis, M. L., Williams, O., Palomero, T., Tosello, V., Pallikuppam, S., Real, P. J., Barnes, K., Zuurbier, L., Meijerink, J. P., and Ferrando, A. A. (2008). NOTCH1 extracellular juxtamembrane expansion mutations in T-ALL. Blood *112*, 733-740.

Thompson, B. J., Buonamici, S., Sulis, M. L., Palomero, T., Vilimas, T., Basso, G., Ferrando, A., and Aifantis, I. (2007). The SCFFBW7 ubiquitin ligase complex as a tumor suppressor in T cell leukemia. J Exp Med *204*, 1825-1835.

Thurston, G., Noguera-Troise, I., and Yancopoulos, G. D. (2007). The Delta paradox: DLL4 blockade leads to more tumour vessels but less tumour growth. Nat Rev Cancer *7*, 327-331.

van Dongen, J. J., Langerak, A. W., Bruggemann, M., Evans, P. A., Hummel, M., Lavender, F. L., Delabesse, E., Davi, F., Schuuring, E., Garcia-Sanz, R.*, et al.* (2003). Design and standardization of PCR primers and protocols for detection of clonal immunoglobulin and T-cell receptor gene recombinations in suspect lymphoproliferations: report of the BIOMED-2 Concerted Action BMH4-CT98-3936. Leukemia *17*, 2257-2317.

van Dongen, J. J., Macintyre, E. A., Gabert, J. A., Delabesse, E., Rossi, V., Saglio, G., Gottardi, E., Rambaldi, A., Dotti, G., Griesinger, F.*, et al.* (1999). Standardized RT-PCR analysis of fusion gene transcripts from chromosome aberrations in acute leukemia for detection of minimal residual disease. Report of the BIOMED-1 Concerted Action: investigation of minimal residual disease in acute leukemia. Leukemia *13*, 1901-1928.

Weng, A. P., Ferrando, A. A., Lee, W., Morris, J. P. t., Silverman, L. B., Sanchez-Irizarry, C., Blacklow, S. C., Look, A. T., and Aster, J. C. (2004). Activating mutations of NOTCH1 in human T cell acute lymphoblastic leukemia. Science *306*, 269-271.

Weng, A. P., Millholland, J. M., Yashiro-Ohtani, Y., Arcangeli, M. L., Lau, A., Wai, C., Del Bianco, C., Rodriguez, C. G., Sai, H., Tobias, J.*, et al.* (2006). c-Myc is an important direct target of Notch1 in T-cell acute lymphoblastic leukemia/lymphoma. Genes Dev *20*, 2096-2109.

Wilson, A., MacDonald, H. R., and Radtke, F. (2001). Notch 1-deficient common lymphoid precursors adopt a B cell fate in the thymus. J Exp Med *194*, 1003-1012.

Wu, Y., Cain-Hom, C., Choy, L., Hagenbeek, T. J., de Leon, G. P., Chen, Y., Finkle, D., Venook, R., Wu, X., Ridgway, J.*, et al.* (2010). Therapeutic antibody targeting of individual Notch receptors. Nature *464*, 1052-1057.

Zhang, J., Ding, L., Holmfeldt, L., Wu, G., Heatley, S. L., Payne-Turner, D., Easton, J., Chen, X., Wang, J., Rusch, M.*, et al.* (2012). The genetic basis of early T-cell precursor acute lymphoblastic leukaemia. Nature *481*, 157-163.

Zhang, Y., Li, B., Ji, Z. Z., and Zheng, P. S. (2010). Notch1 regulates the growth of human colon cancers. Cancer *116*, 5207-5218.